Physics of Accretion Disks

Wladimir Lyra

California State University

Jet Propulsion Laboratory

Moscow Institute of Physics and Technology, Jul 3rd, 2017

Dead zones

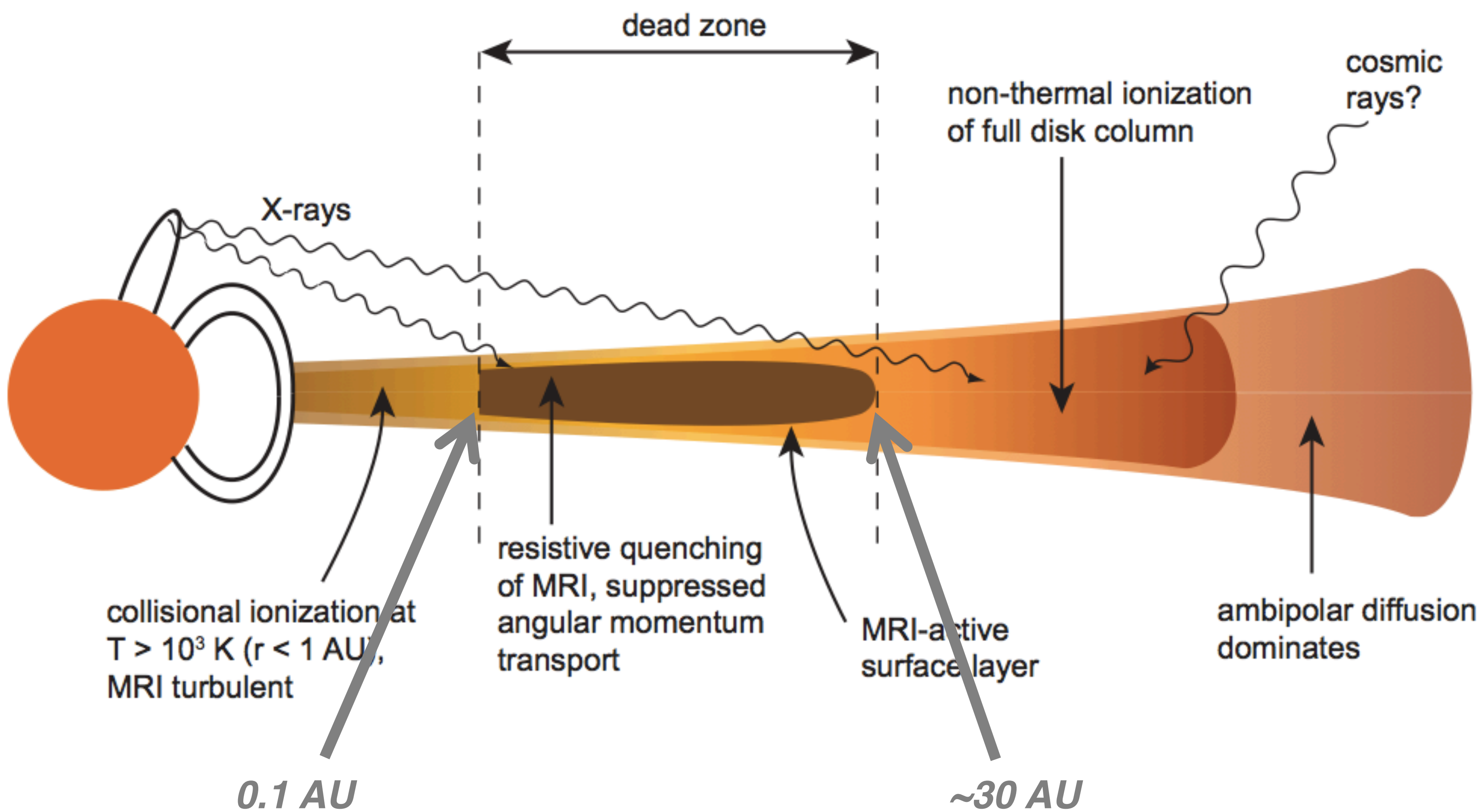

dead zone
non-thermal ionization
of full disk column
cosmic
rays?
X-rays
resistive quenching
of MRI, suppressed
angular momentum
transport
collisional ionization at
T > 10³ K (r < 1 AU),
MRI turbulent
MRI-active
surface layer
ambipolar diffusion
dominates
0.1 AU
~30 AU

Observational Evidence
Oph IRS 48

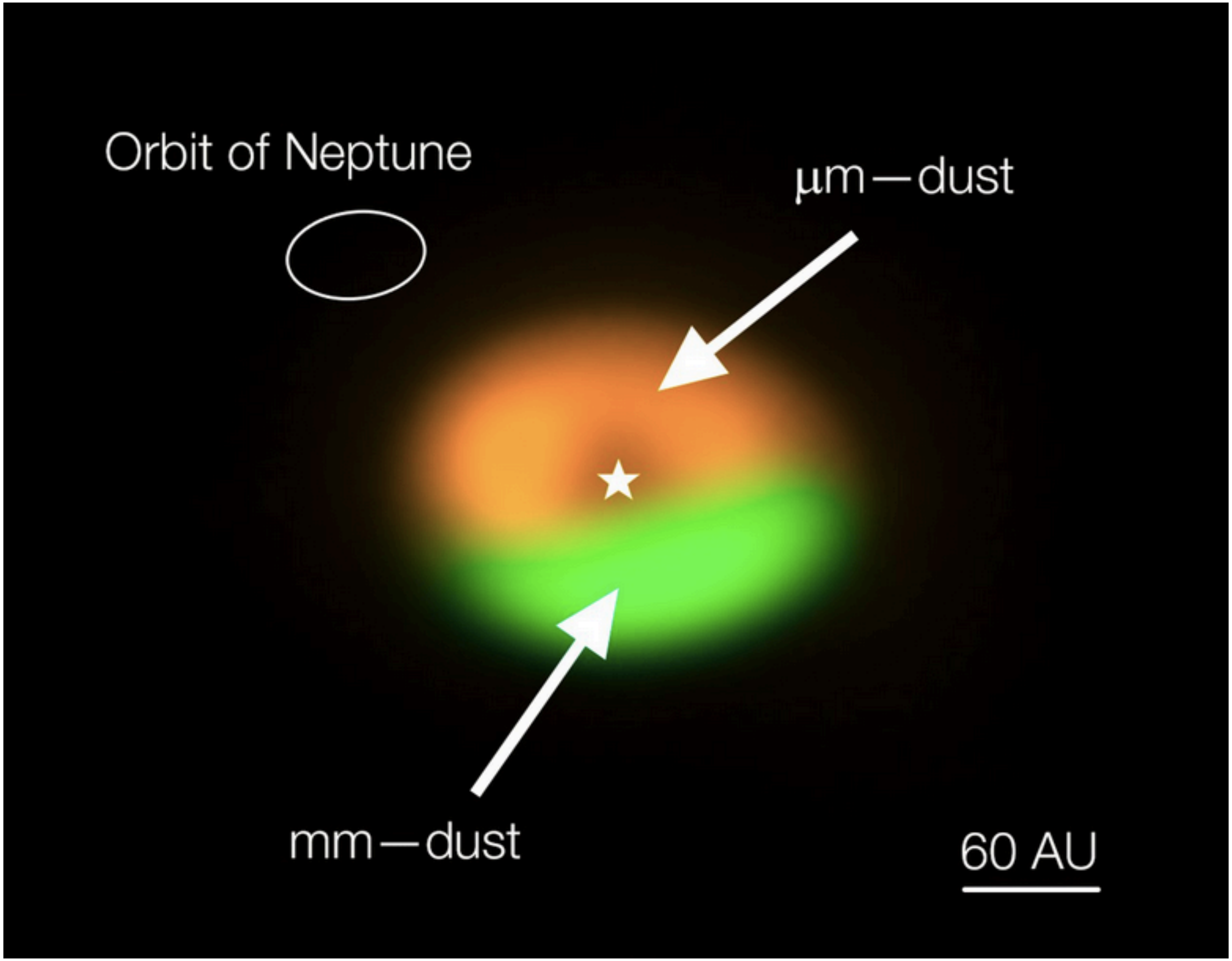

The Oph IRS 48 "dust trap"

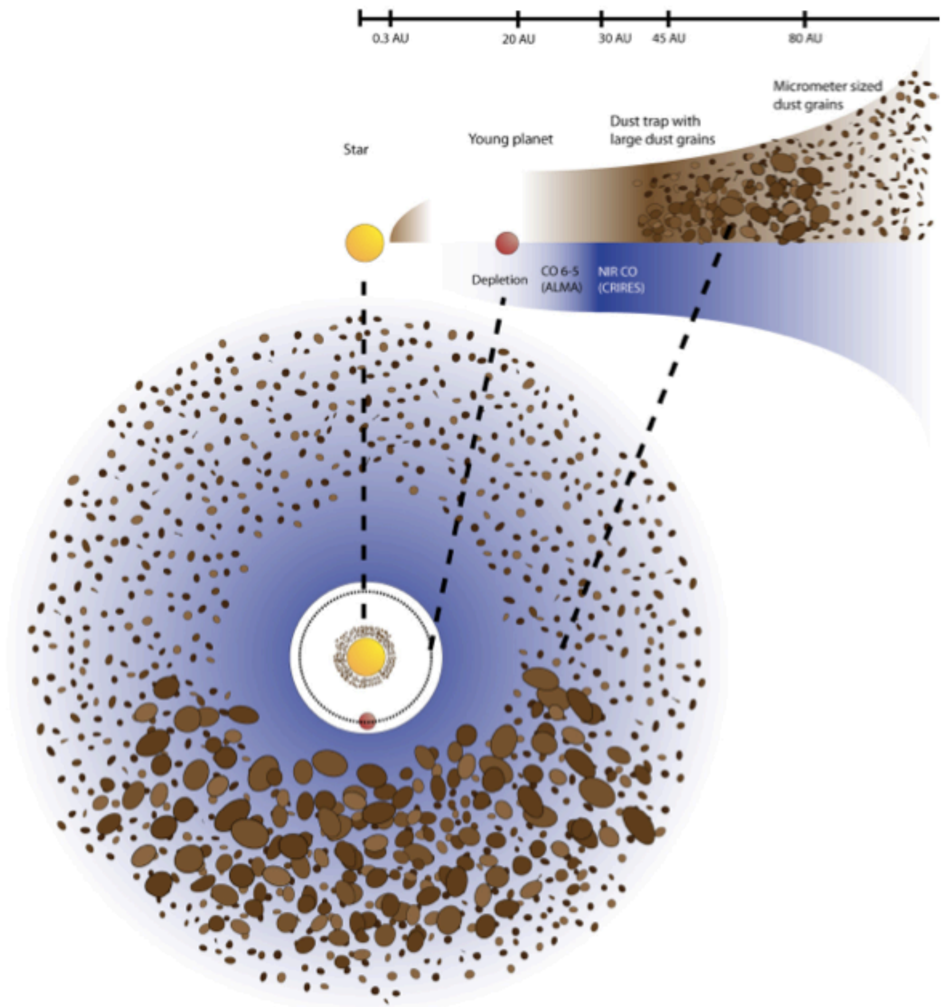

van der Marel et al. (2013)

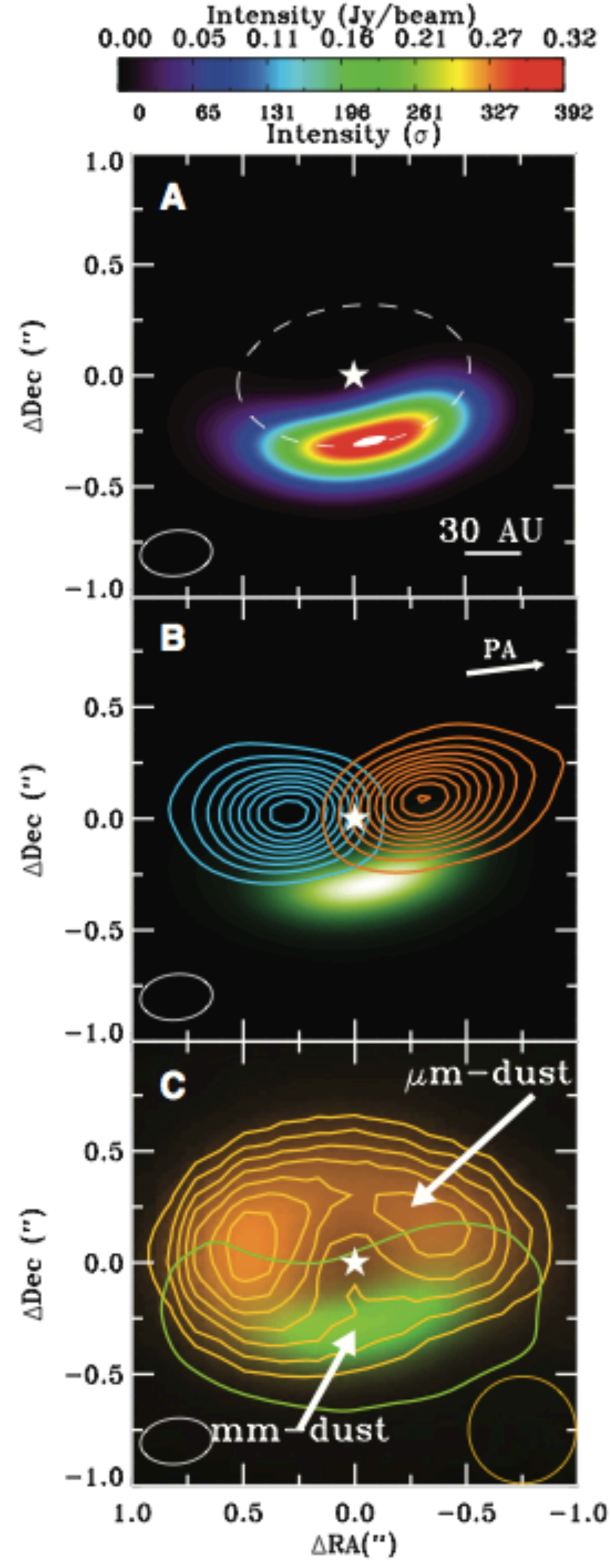

asymmetric mm dust at 63 AU

Gas detection: Keplerian rotation

Micron-sized dust follows gas

Other “asymmetries”

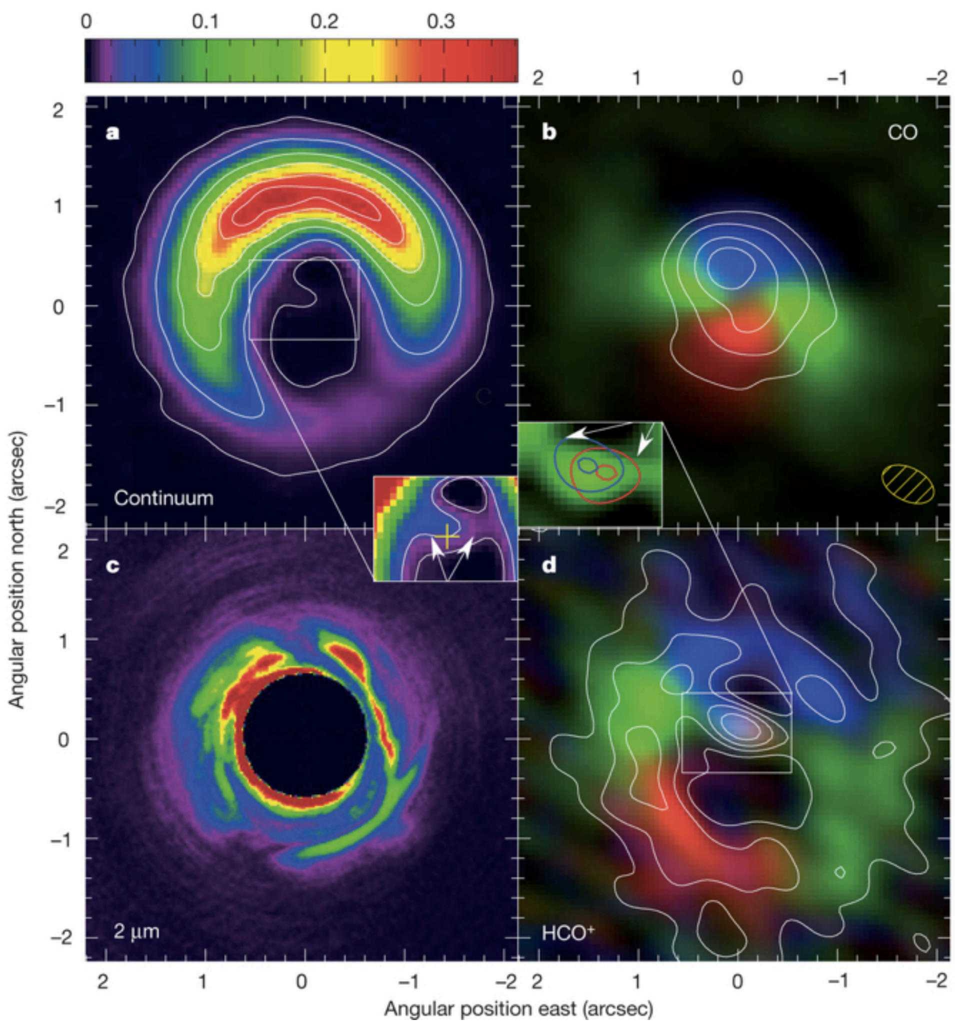

Casassus et al. (2013)

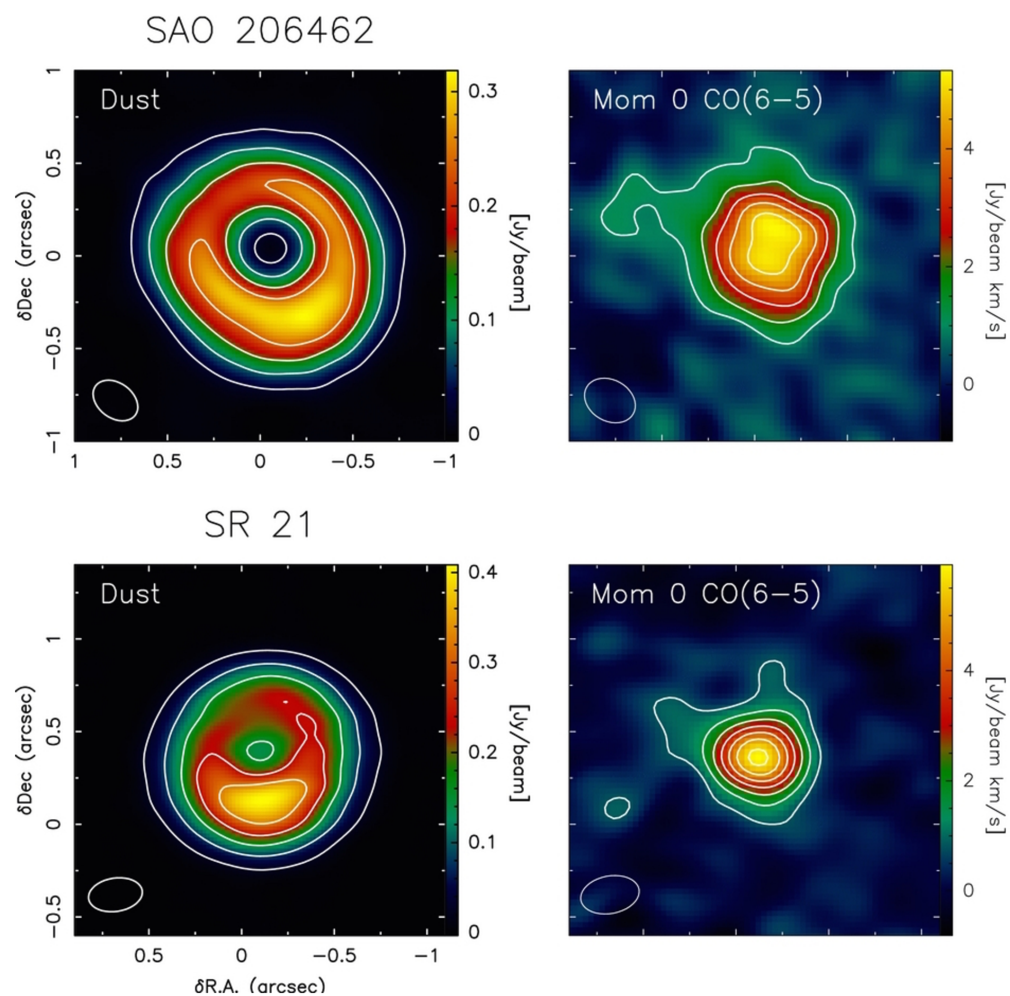

Perez et al. (2014)

“Asymmetries” everywhere

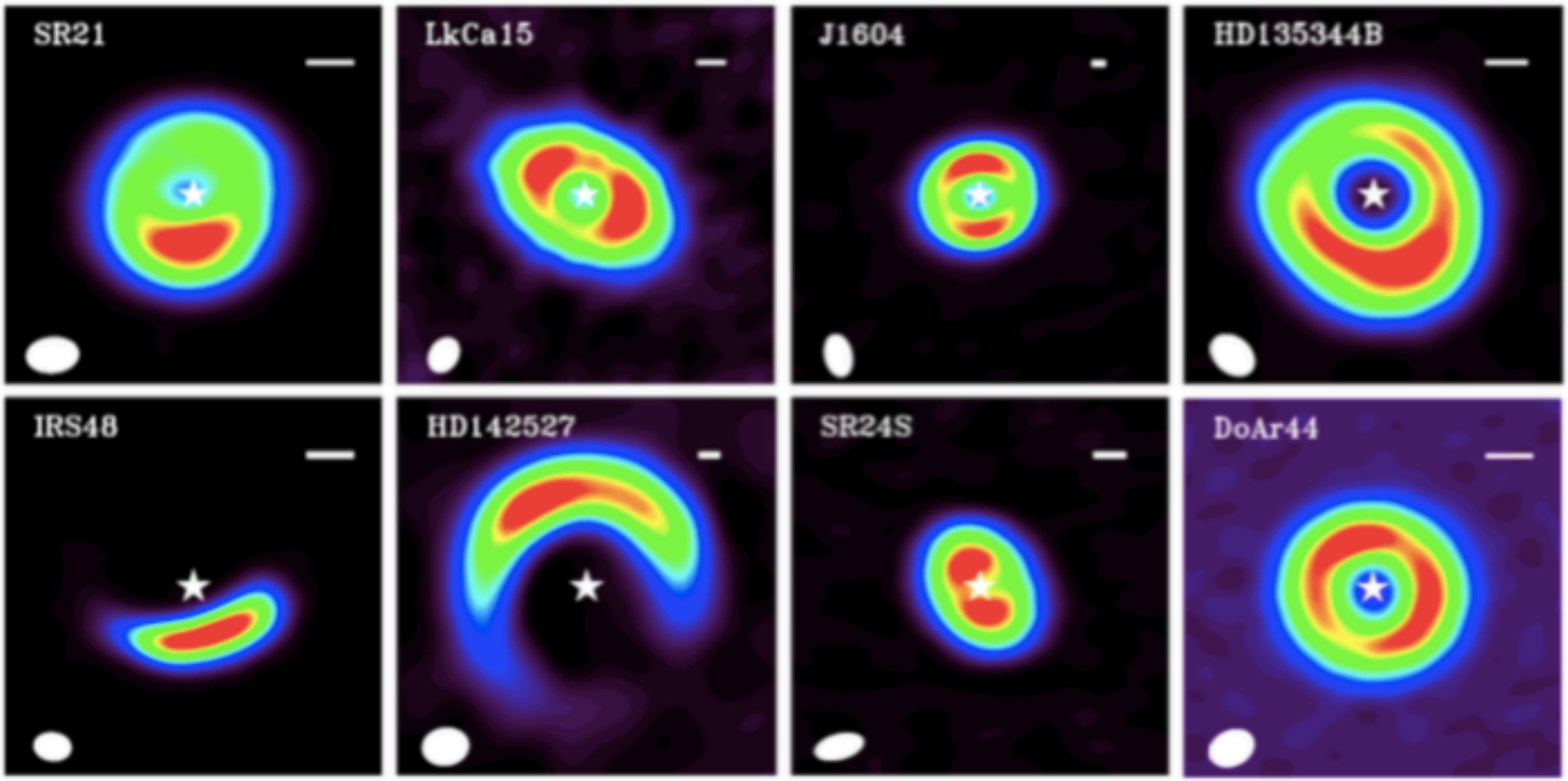

Vortices – an ubiquitous fluid mechanics phenomenon

Von Kármán *vortex street*

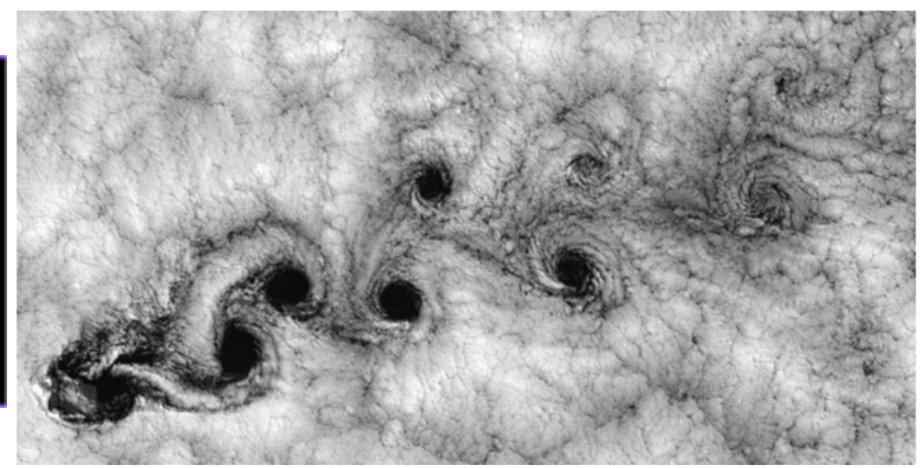

A simple dead zone model

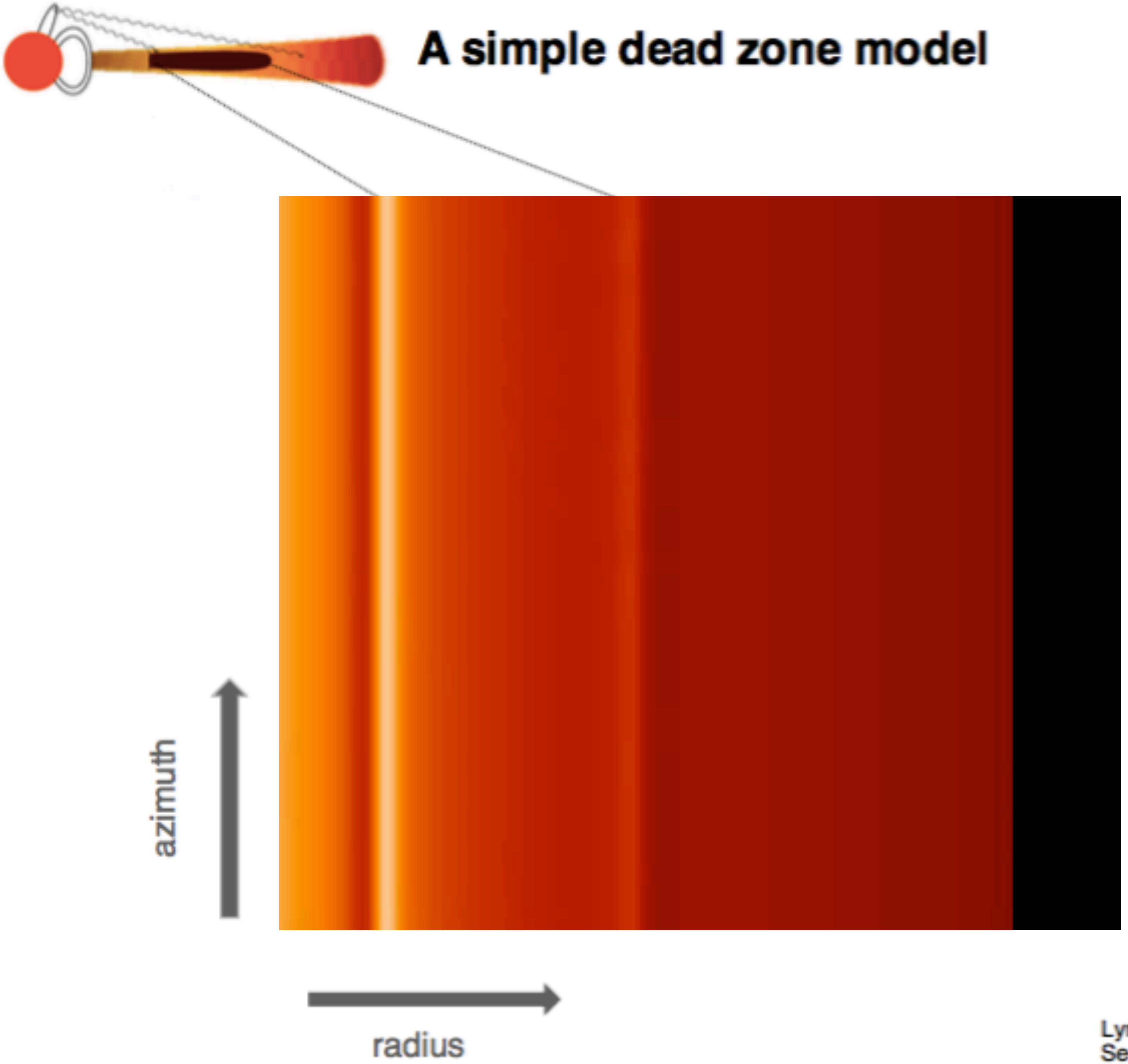

Lyra et al. (2008b, 2009a);
See also Varniere & Tagger (2006)

Rossby wave instability

(or… Kelvin-Helmholtz in differentially rotating disks)

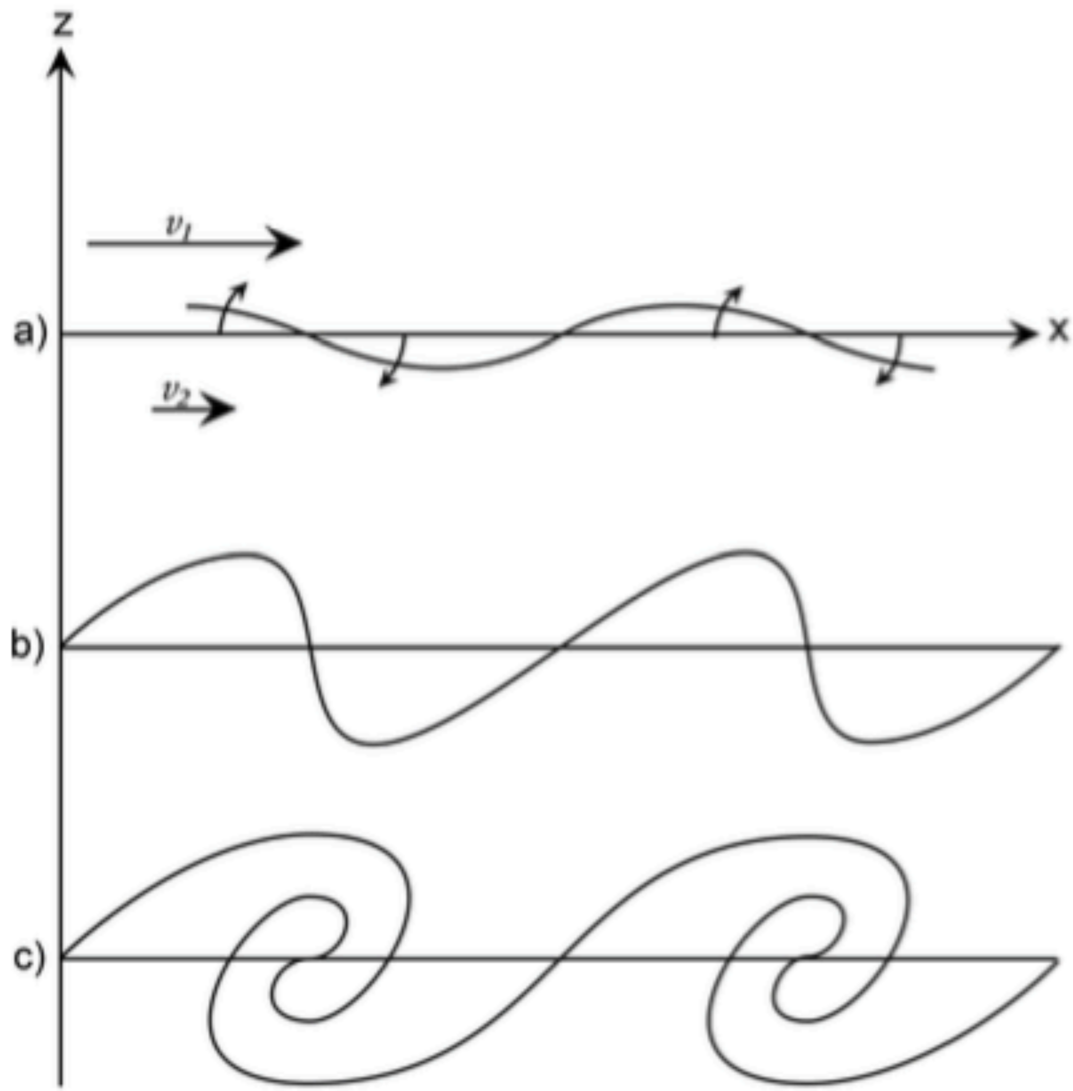

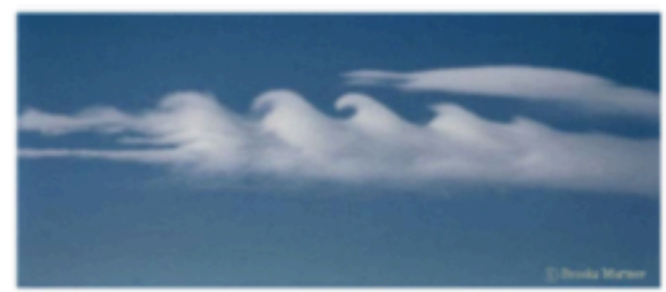

Inner (0.1 AU) active/dead zone boundary

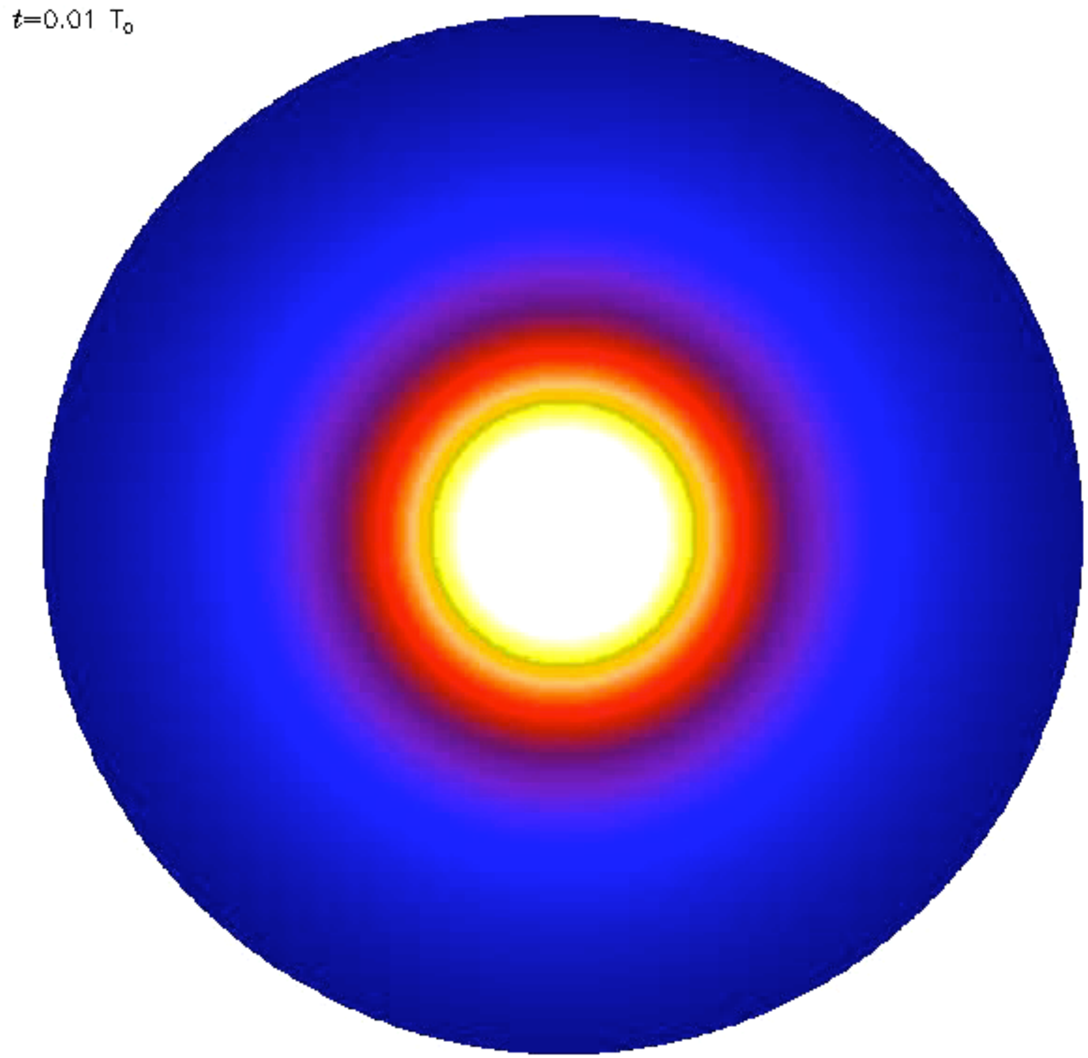

Magnetized inner disk + resistive outer disk

Lyra & Mac Low (2012)

Active/dead zone boundary

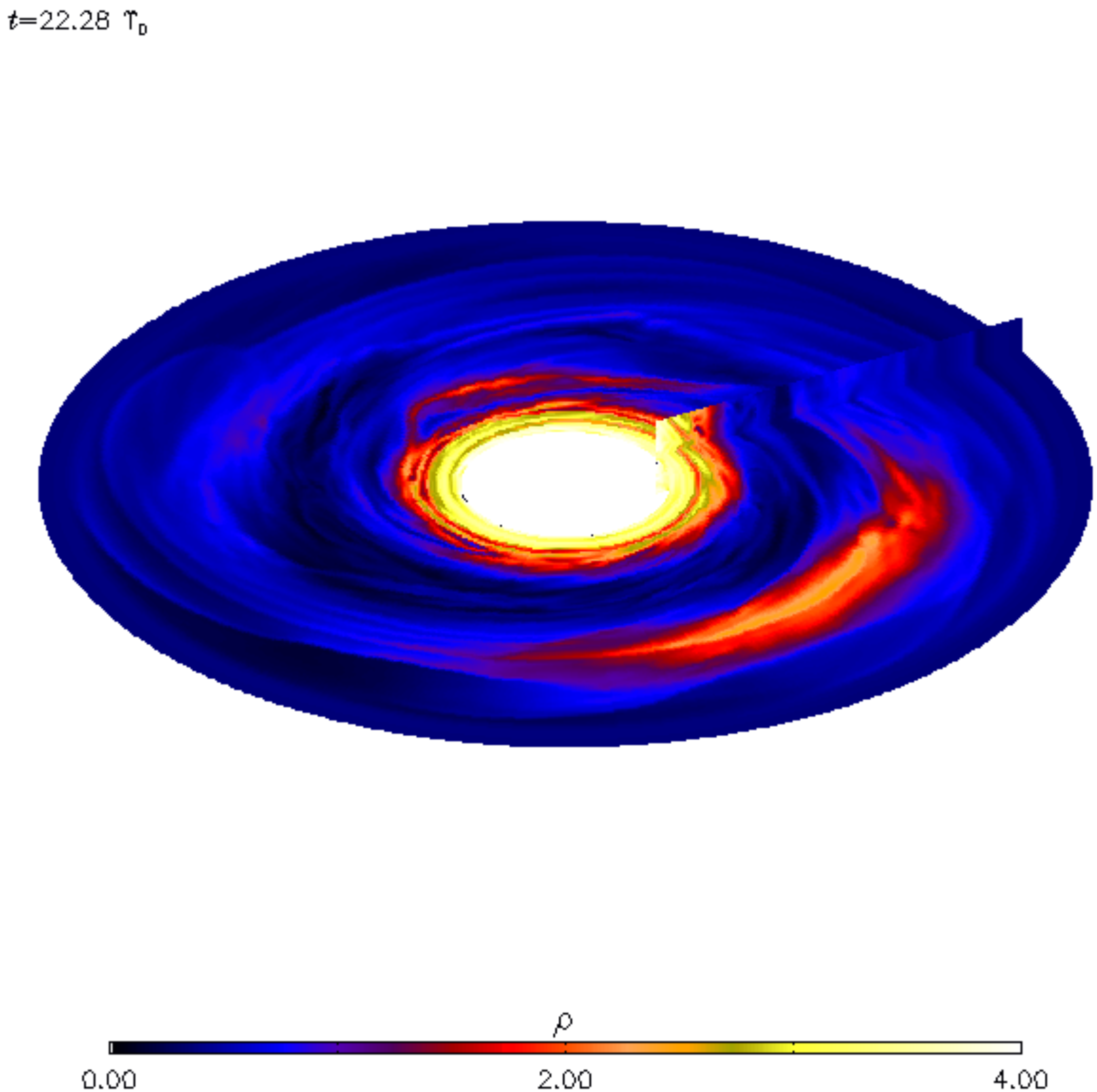

Magnetized inner disk + resistive outer disk

Lyra & Mac Low (2012)

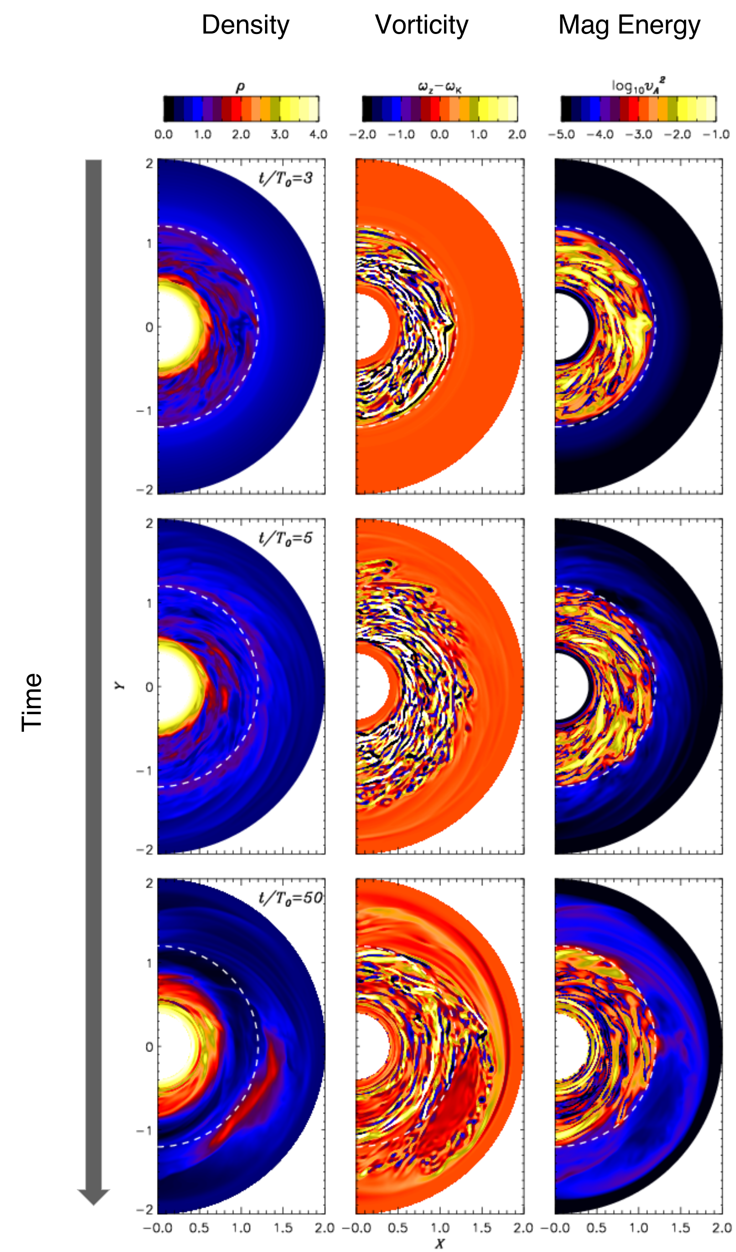

Outer Dead/Active zone transition: 3D MHD

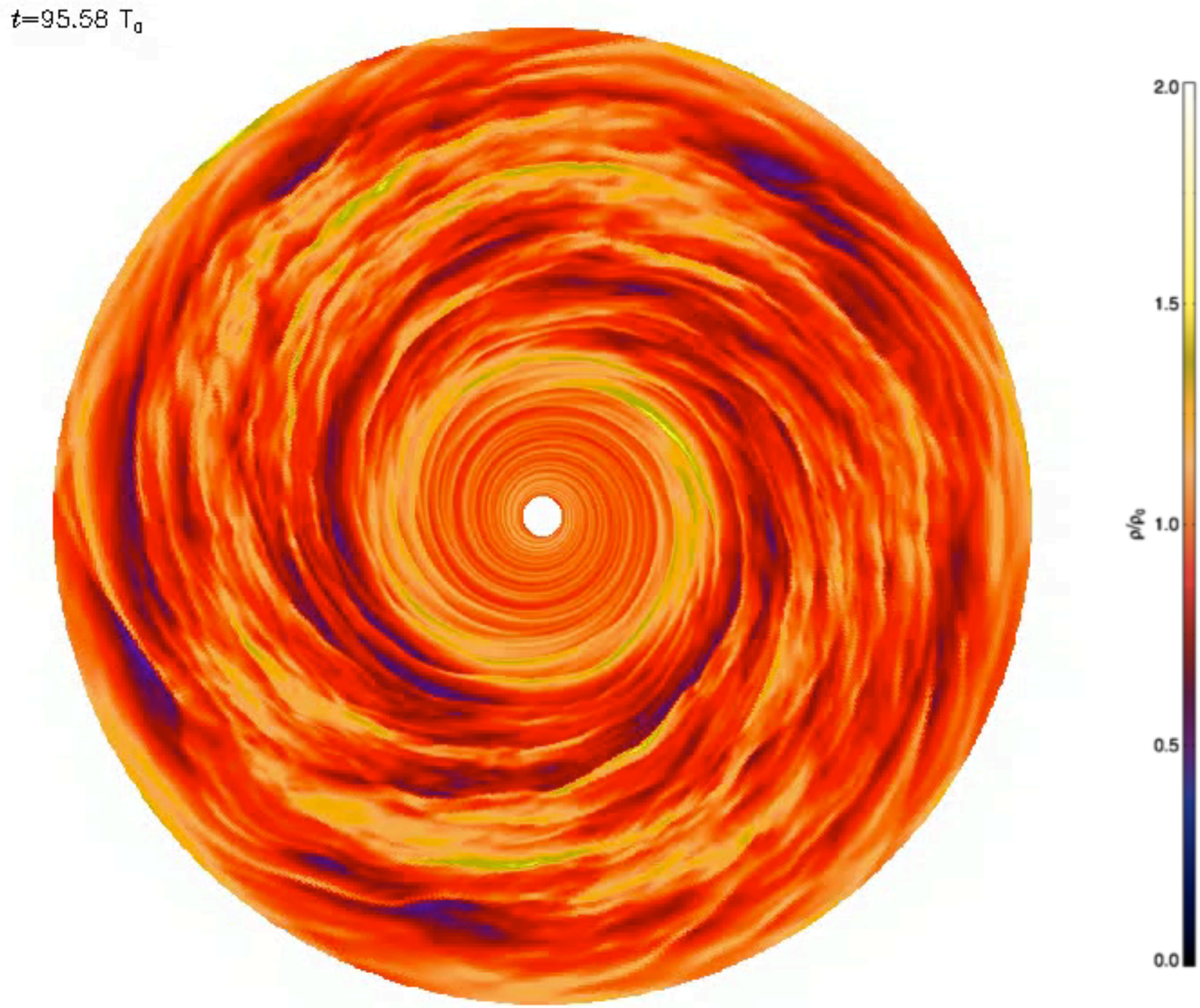

Resistive inner disk + magnetized outer disk

Lyra, Turner, & McNally (2015)

Outer Dead/Active zone transition KHI

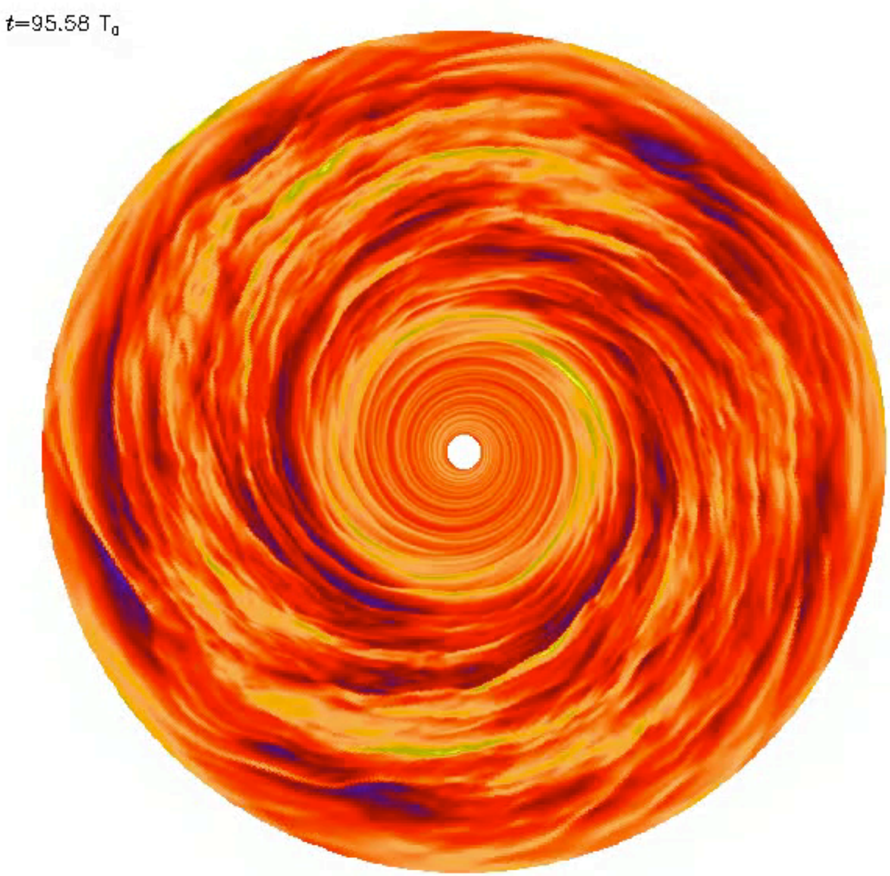

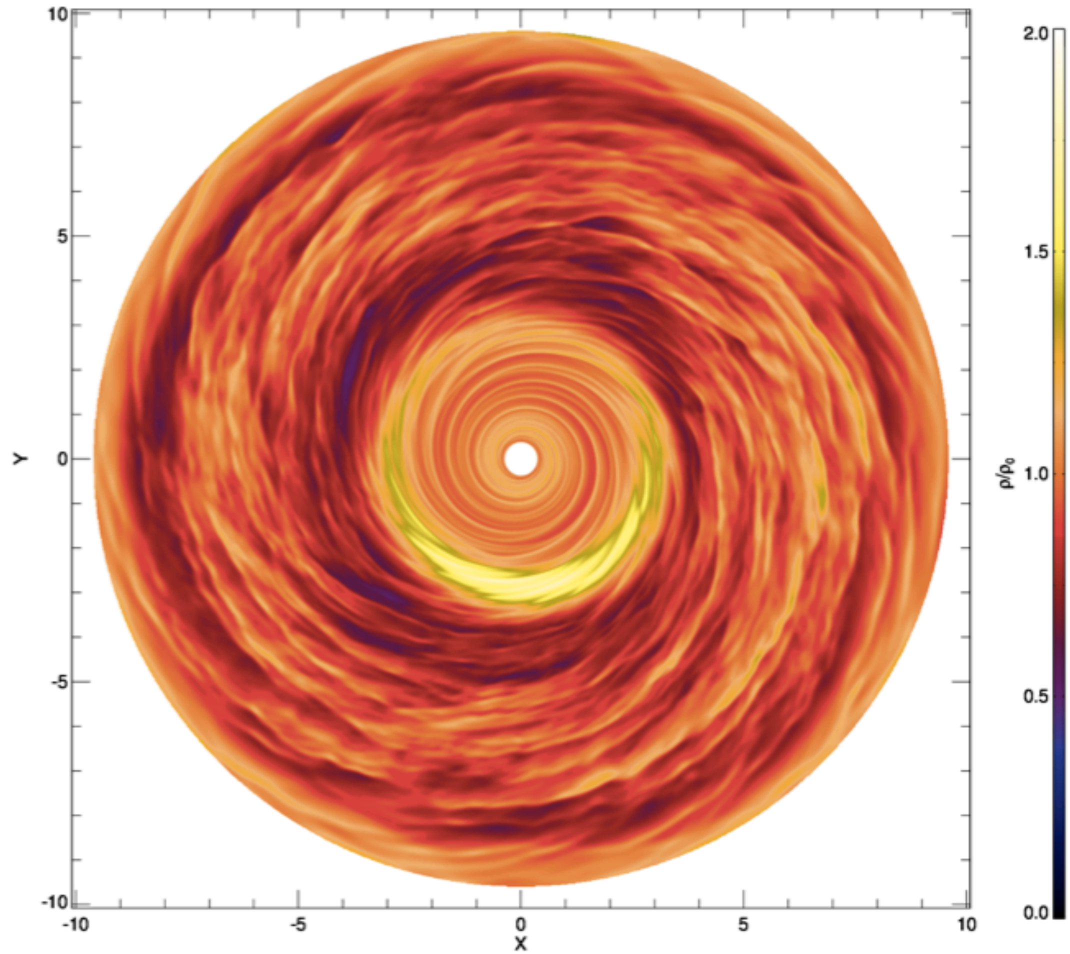

Resistive inner disk + magnetized outer disk

Lyra, Turner, & McNally (2015)

Dust Trapping: The Tea-Leaf Effect

Geostrophic balance:

$$2\Omega \times \boldsymbol{u} = -\rho^{-1} \nabla p$$

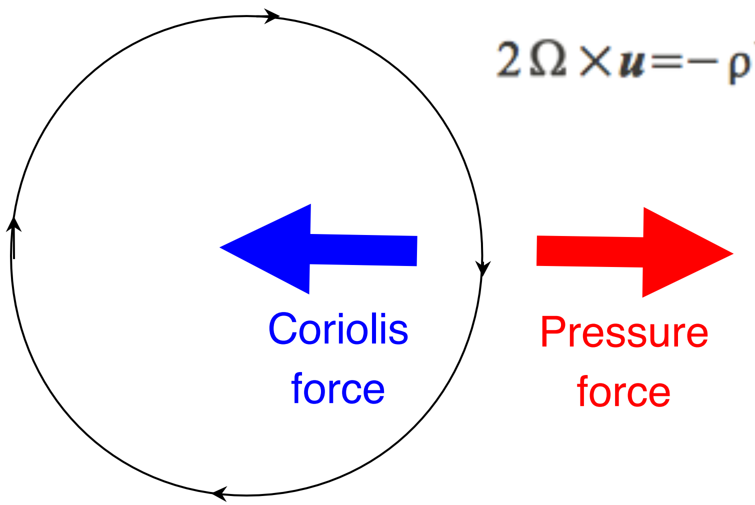

Vortex streamline

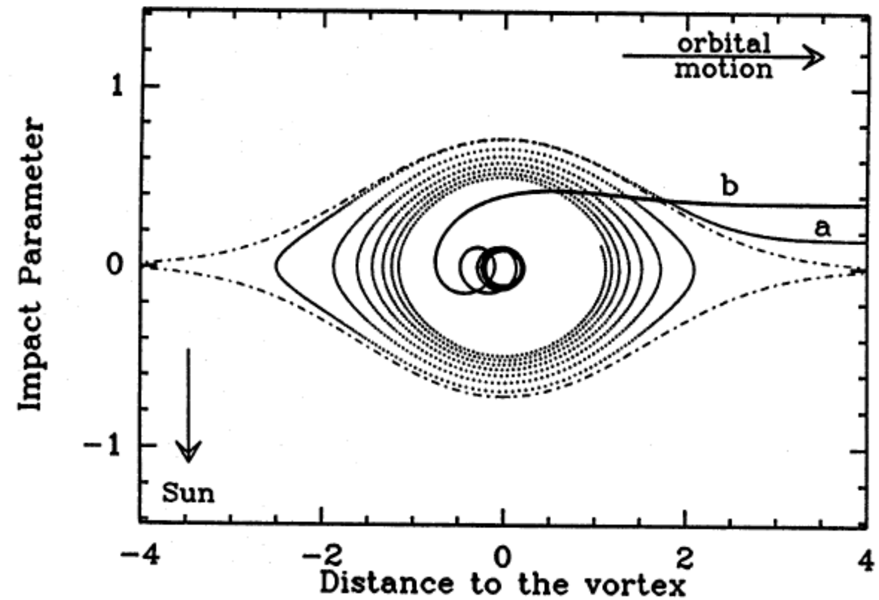

Barge & Sommeria (1995)

Grains do not feel the pressure gradient.
They sink towards the center, where they accumulate.

Drag-Diffusion Equilibrium

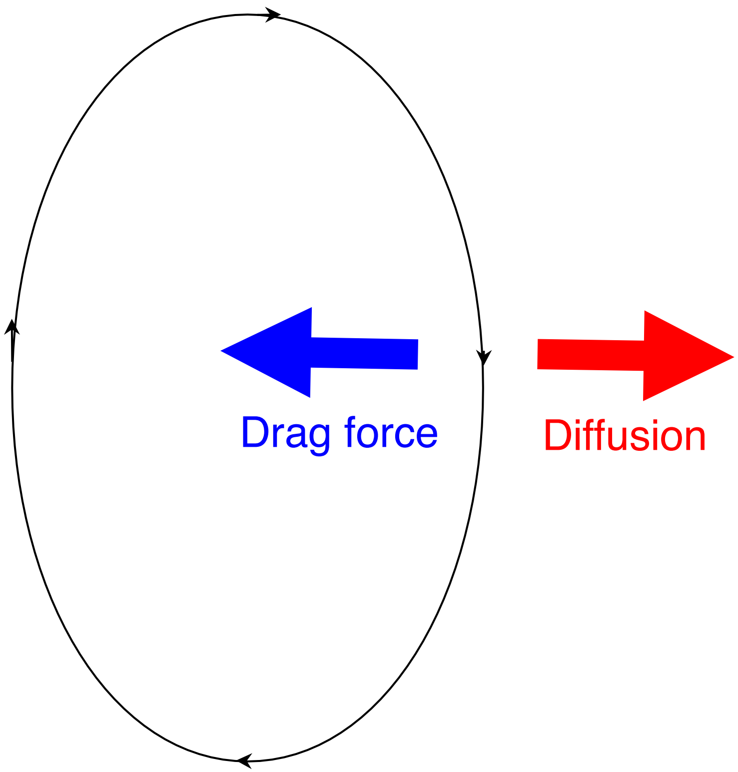

Trapped particle

Dust continuity equation

$$\frac{\partial \rho_d}{\partial t} = \underbrace{-(\boldsymbol{v} \cdot \boldsymbol{\nabla})\rho_d}_{\text{advection}} \underbrace{- \rho_d \boldsymbol{\nabla} \cdot \boldsymbol{v}}_{\text{compression}} + \underbrace{D\nabla^2\rho_d}_{\text{diffusion}},$$

Drag-Diffusion Equilibrium

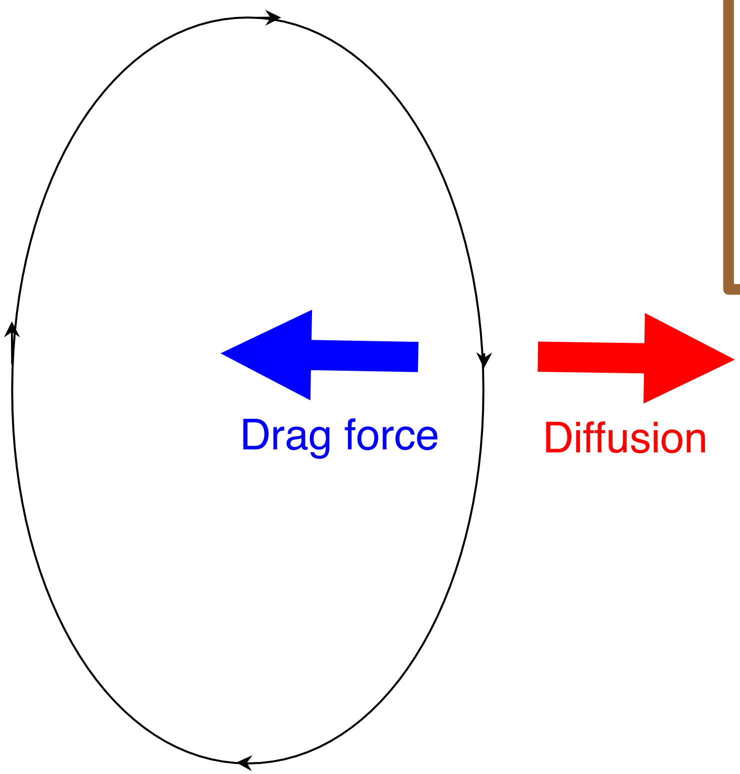

Trapped particle

Steady-state solution

$$\rho_d(a,z) = \varepsilon\rho_0 (S+1)^{3/2} \exp\left\{-\frac{[a^2 f^2(\chi)+z^2]}{2H^2}(S+1)\right\}$$

Lyra & Lin (2013)

$$S = \frac{St}{\delta}$$

$$\delta = v_{\mathrm{rms}}^2 / c_s^2,$$

a = vortex semi-minor axis
H = disk scale height (temperature)
χ = vortex aspect ratio
δ = diffusion parameter
St = Stokes number (particle size)
$f(\chi)$ = model-dependent scale function

Analytical solution for dust trapping

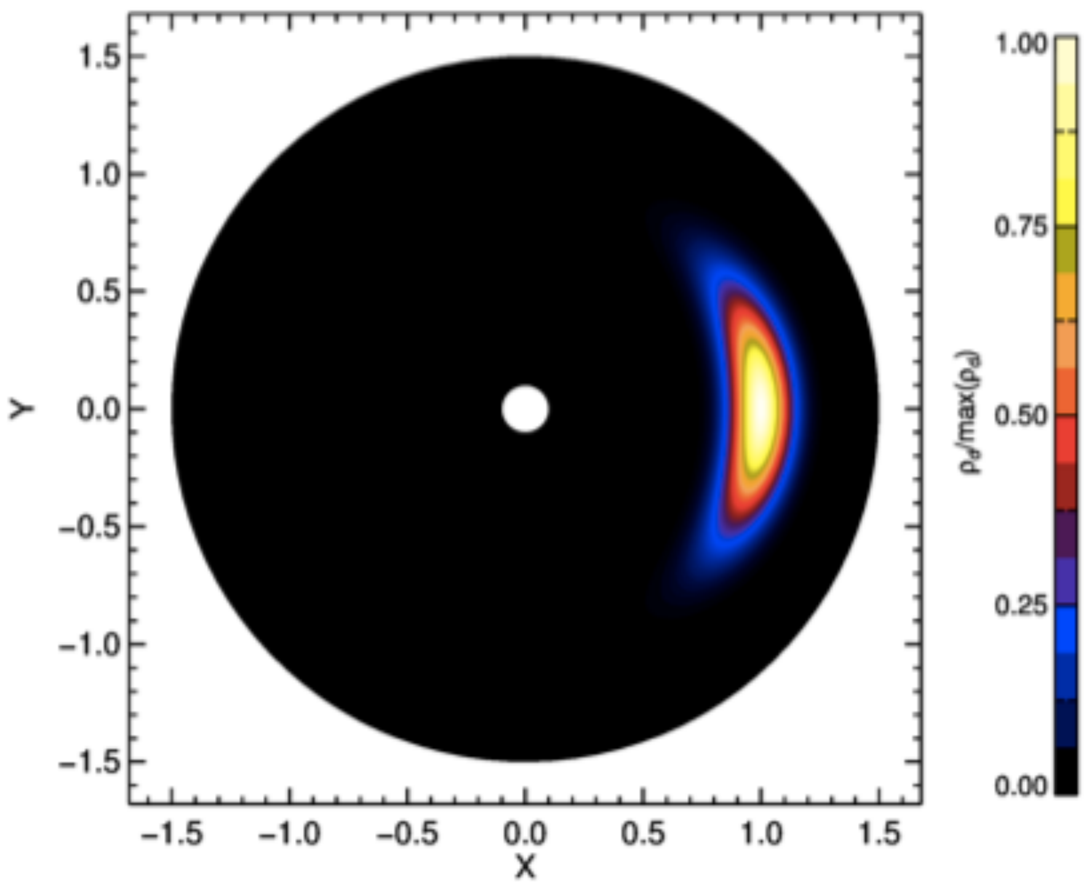

Solution

$$\rho_d(a) = \rho_{d\,\max} \exp\left(-\frac{a^2}{2H_V^2}\right),$$

$$H_V = \frac{H}{f(\chi)}\sqrt{\frac{1}{S+1}}$$

$$S = \frac{St}{\delta}$$

$$\delta = v_{\rm rms}^2/c_s^2,$$

Solution for

$H/r=0.1$ $\chi=4$ $S=1$

a = vortex semi-minor axis
H = disk scale height (temperature)
χ = vortex aspect ratio
δ = diffusion parameter
St = Stokes number (particle size)
$f(\chi)$ = model-dependent scale function

Lyra & Lin (2013)

Analytical vs Numerical

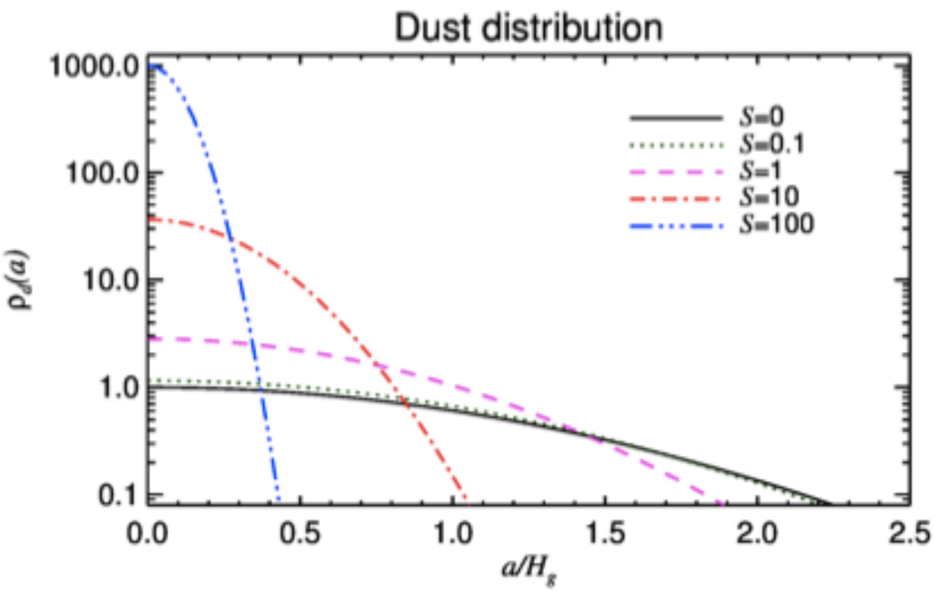

$$S = \frac{St}{\delta} \qquad \delta = v_{\rm rms}^2 / c_s^2,$$

Lyra & Lin (2013)

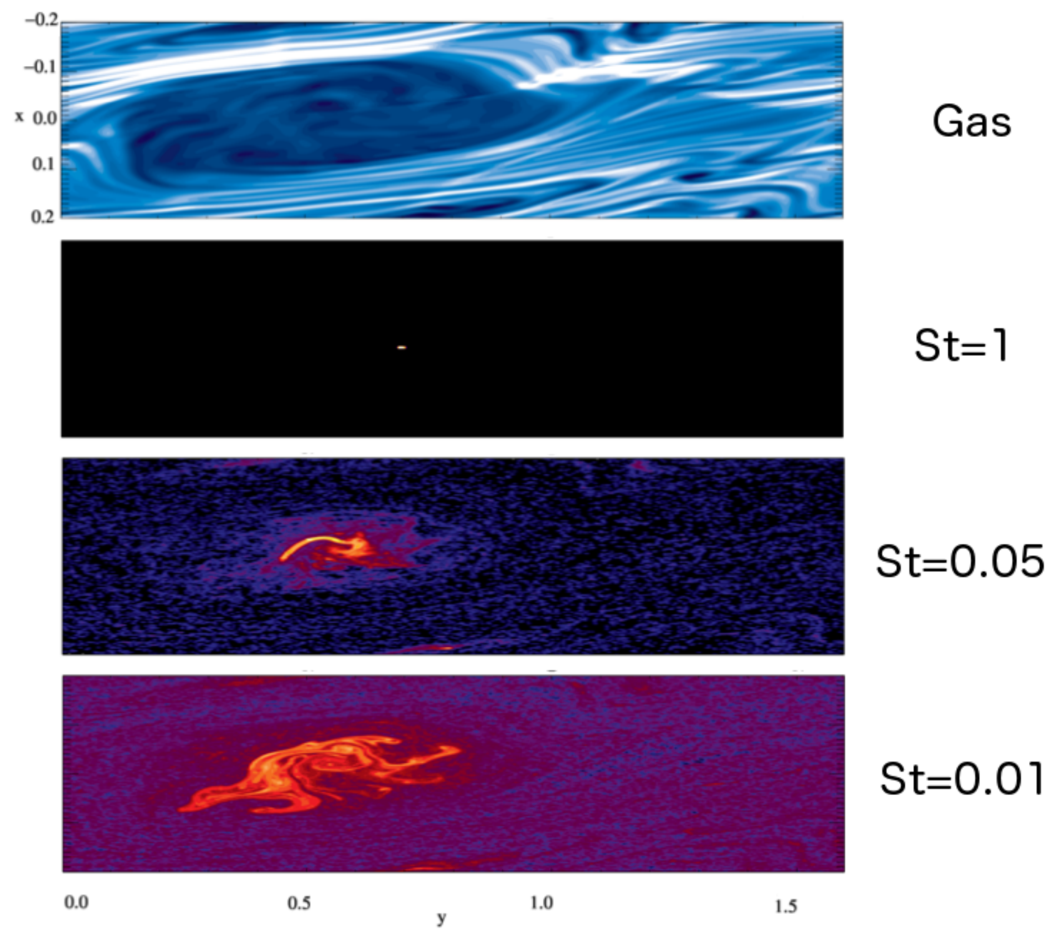

Raettig et al (2015)

Derived quantities

$$\rho_d(a,z) = \varepsilon\rho_0 (S+1)^{3/2} \exp\left\{-\frac{[a^2 f^2(\chi)+z^2]}{2H^2}(S+1)\right\}$$

Lyra & Lin (2013)

Gas distribution

$$\rho_g(a) = \rho_{g\,\max} \exp\left(-\frac{a^2}{2H_g^2}\right),$$

Maximum dust density

$$\rho_{d\,\max} = \varepsilon\,\rho_0\,(S+1)^{3/2}$$

Gas contrast

$$\frac{\rho_{g\,\max}}{\rho_{g\,\min}} = \exp\left[\frac{f^2(\chi)}{2\chi^2\omega_V^2}\right],$$

Dust contrast

$$\frac{\rho_{d\,\max}}{\rho_{d\,\min}} = \frac{\rho_{g\,\max}}{\rho_{g\,\min}} \exp(S),$$

Total trapped mass

$$\int \rho_d(a,z)dV = (2\pi)^{3/2}\,\varepsilon\rho_0\,\chi H H_g^2$$

Vortex size

$$a_s = H(\chi\omega_V)^{-1}$$

H = disk scale height (temperature)
χ = vortex aspect ratio
δ = diffusion parameter
St = Stokes number (particle size)
$f(\chi)$ = model-dependent scale function
ε = dust-to-gas ratio

Applying the model to Oph IRS 48

Observed parameters

Aspect ratio: 3.1

Dust contrast: 130

Temperature: 60K

Trapped mass: 9 M_{Earth}

Derived parameters

S=4.8

Stokes number, St=0.008

$\delta = 0.005$, $v_{rms} = 4\%\ c_s$

Trapped mass: 11 M_{Earth}

Lyra & Lin (2013)

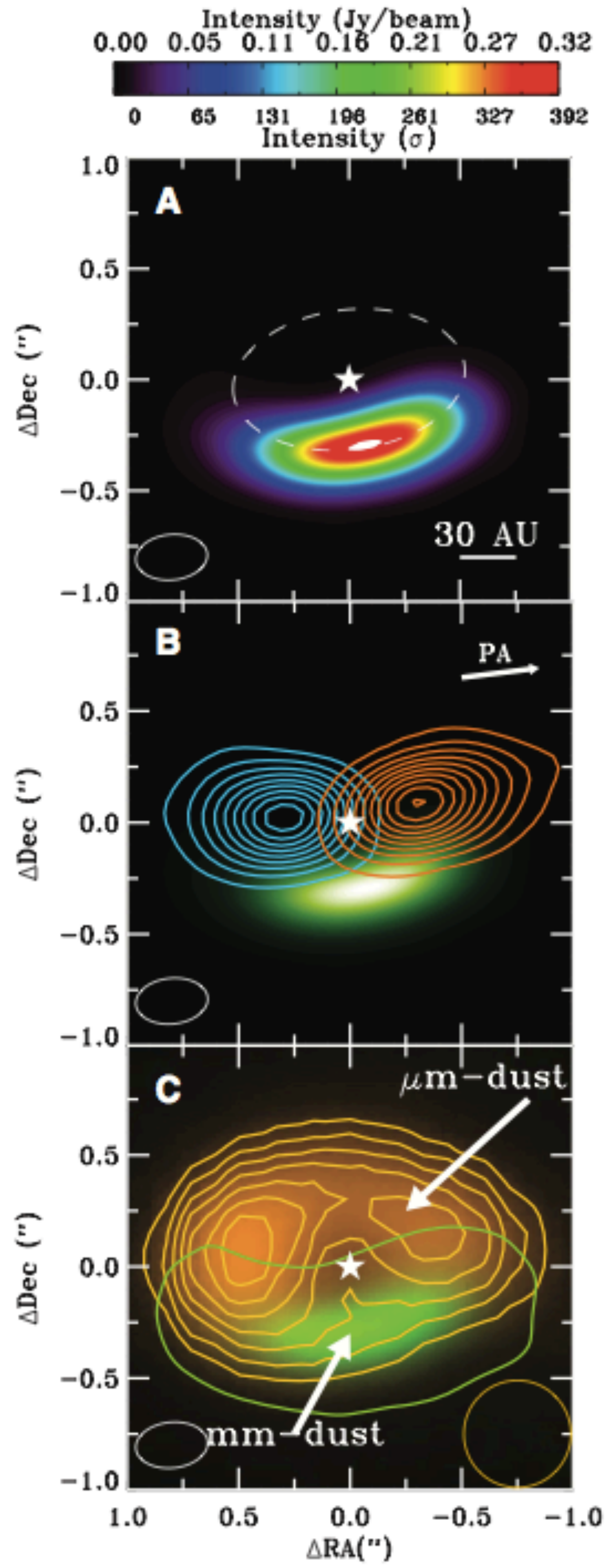

asymmetric mm dust at 63 AU

Gas detection: Keplerian rotation

Micron-sized dust follows gas

Turbulence in vortex cores

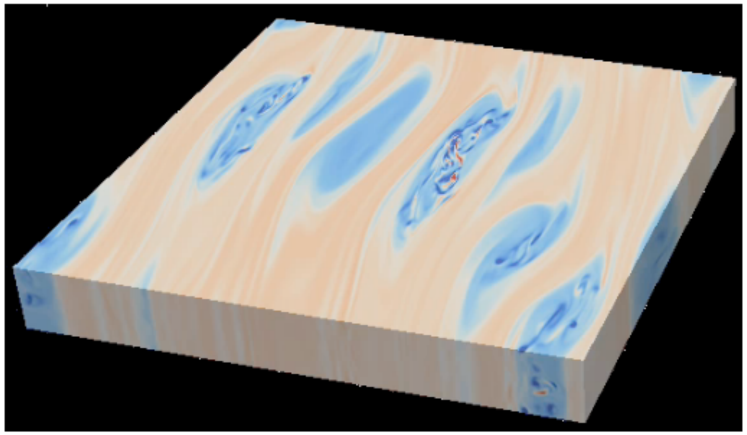

Lesur & Papaloizou (2010)

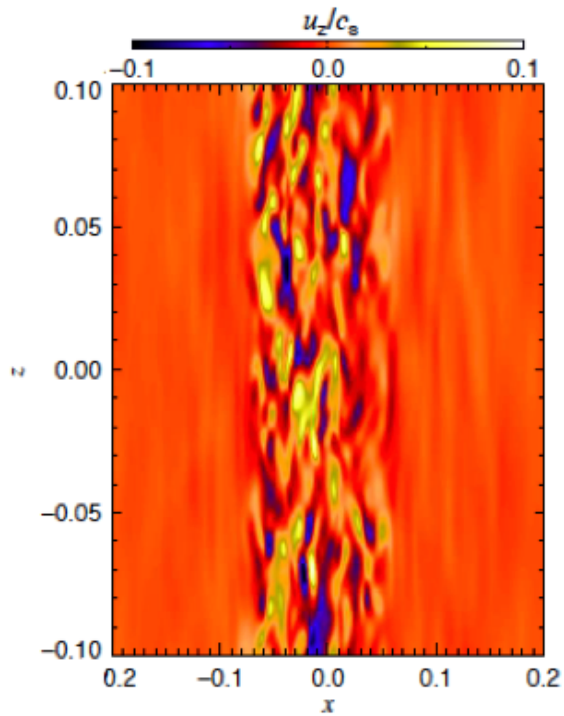

Lyra & Klahr (2011)

Turbulence in vortex cores:

max at ~10% of sound speed
rms at ~3% of sound speed

Vortices in the bulk of the dead zone

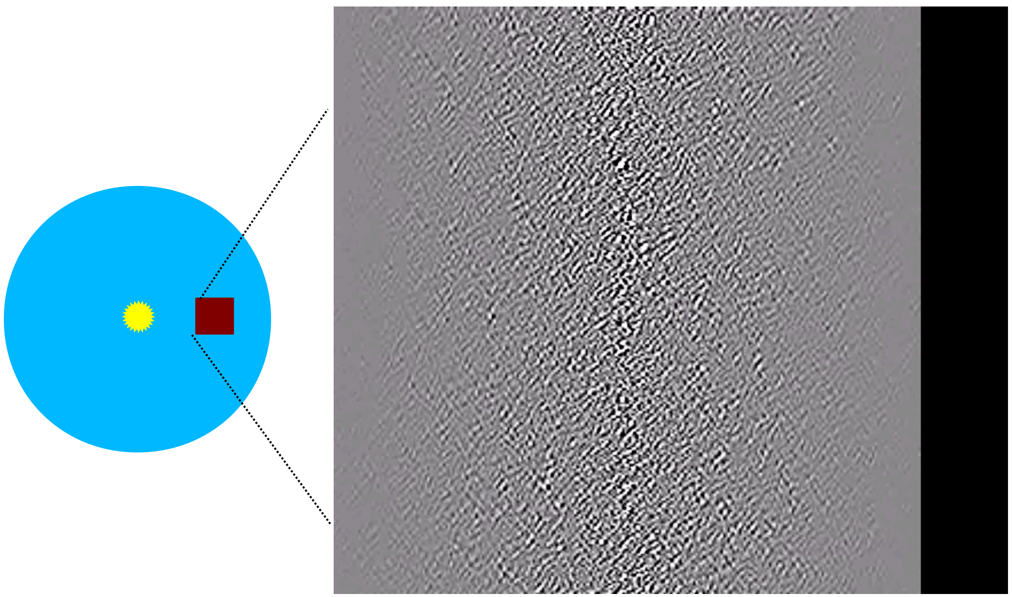

Lyra & Klahr (2011)

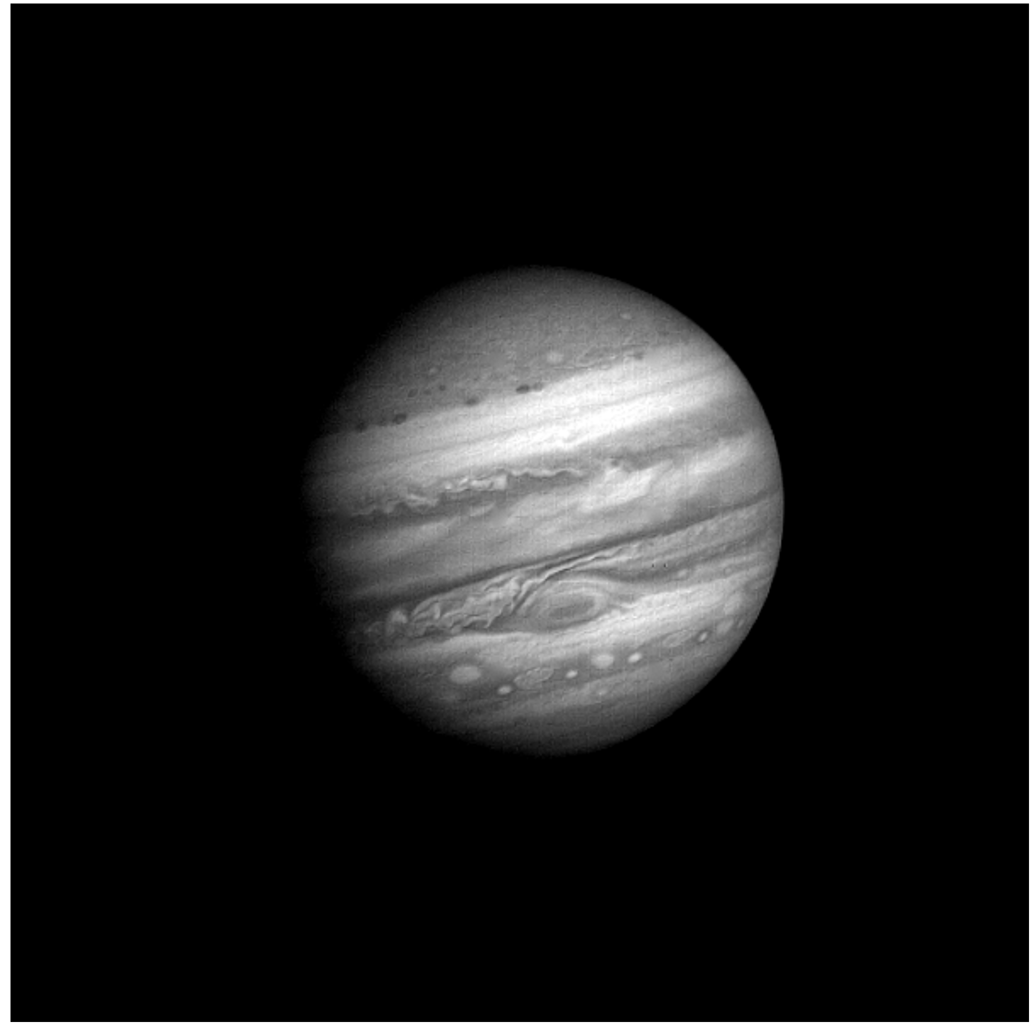

Convective Overstability

Klahr & Hubbard (2014), Lyra (2014), Latter (2015)

$$
\begin{aligned}
\frac{\partial\rho}{\partial t} + (\boldsymbol{u}\cdot\boldsymbol{\nabla})\,\rho &= -\rho\boldsymbol{\nabla}\cdot\boldsymbol{u},\\
\frac{\partial\boldsymbol{u}}{\partial t} + (\boldsymbol{u}\cdot\boldsymbol{\nabla})\,\boldsymbol{u} &= -\frac{1}{\rho}\boldsymbol{\nabla}p + \boldsymbol{g},\\
\frac{\partial p}{\partial t} + (\boldsymbol{u}\cdot\boldsymbol{\nabla})\,p &= -\gamma p\boldsymbol{\nabla}\cdot\boldsymbol{u} - \frac{p}{T}\frac{(T-T_0)}{\tau},
\end{aligned}
$$

$$
\tau_{\max} = \frac{1}{\gamma\Omega};
$$

$$
\sigma_{\max} = -\frac{N^2}{4\Omega}.
$$

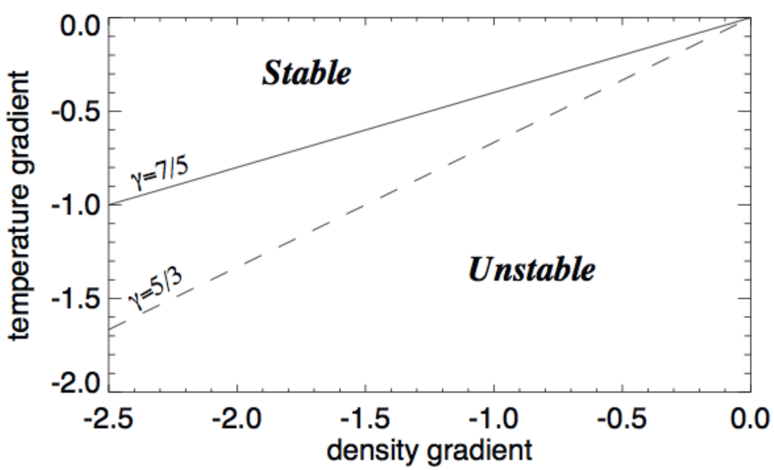

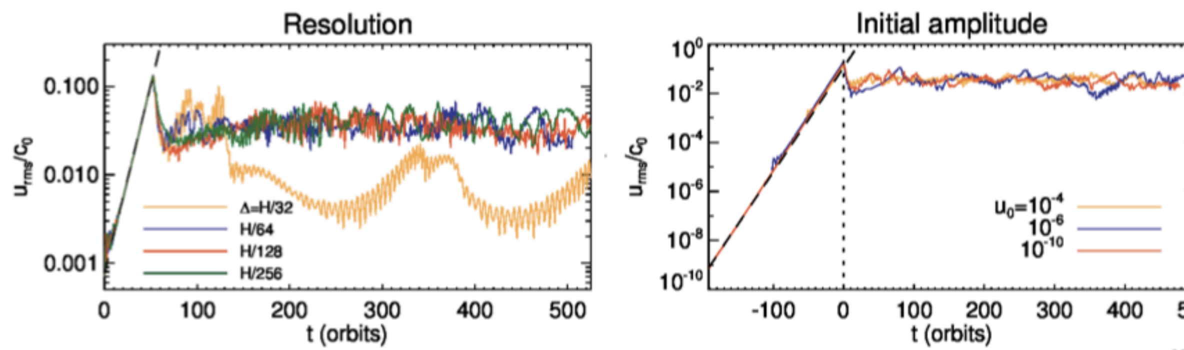

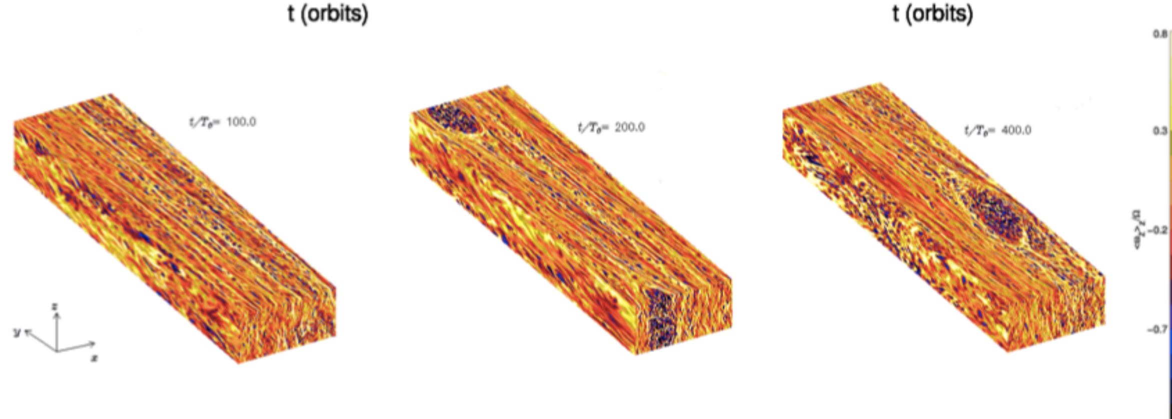

Lyra (2014)

Convective Overstability

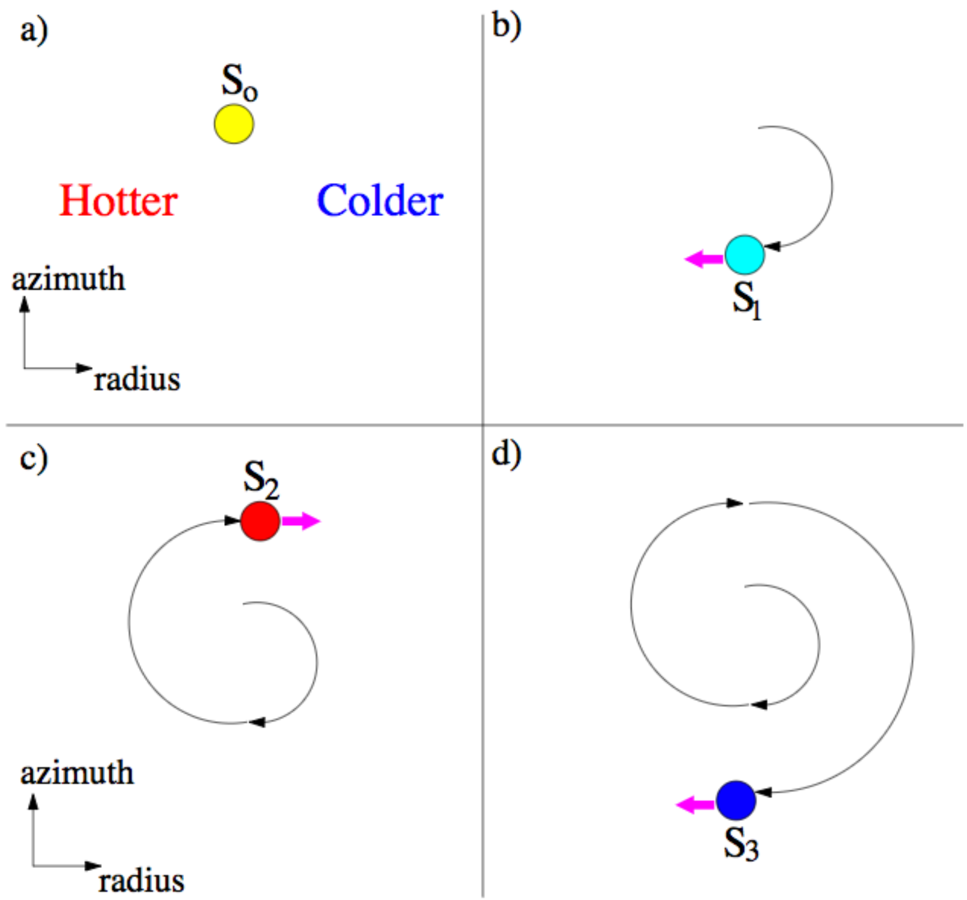

Figure 2. Four panels indicating the convective overstability mechanism. In panel (a) a fluid blob is embedded in a radial entropy gradient. In panel (b) it undergoes half an epicycle and returns to its original radius with a smaller entropy than when it begun $S_1 < S_0$. It hence feels a buoyancy acceleration inwards and the epicycle is amplified. The process occurs in reverse once the epicycle is complete, shown in panel (c), where now $S_2 > S_0$. The oscillations hence grow larger and larger.

Latter (2015)

Convection

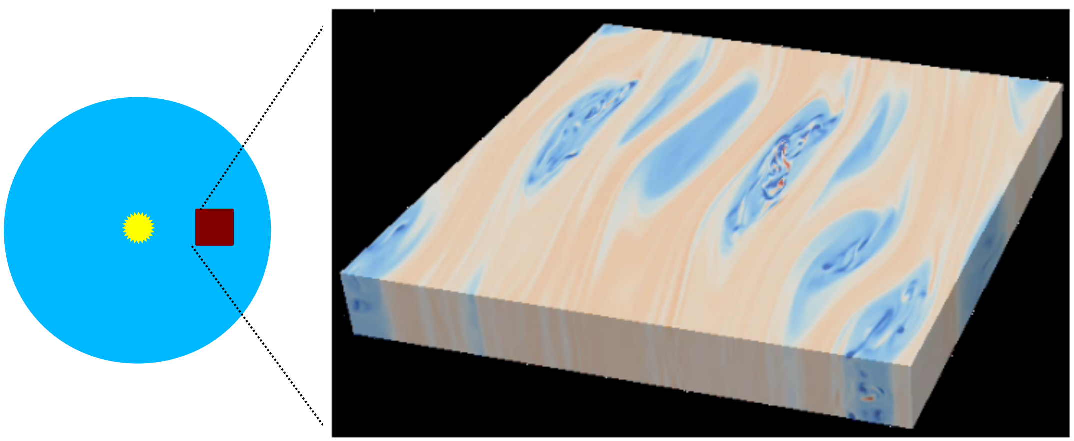

Lesur & Papaloizou (2010)

Sketch of Convection

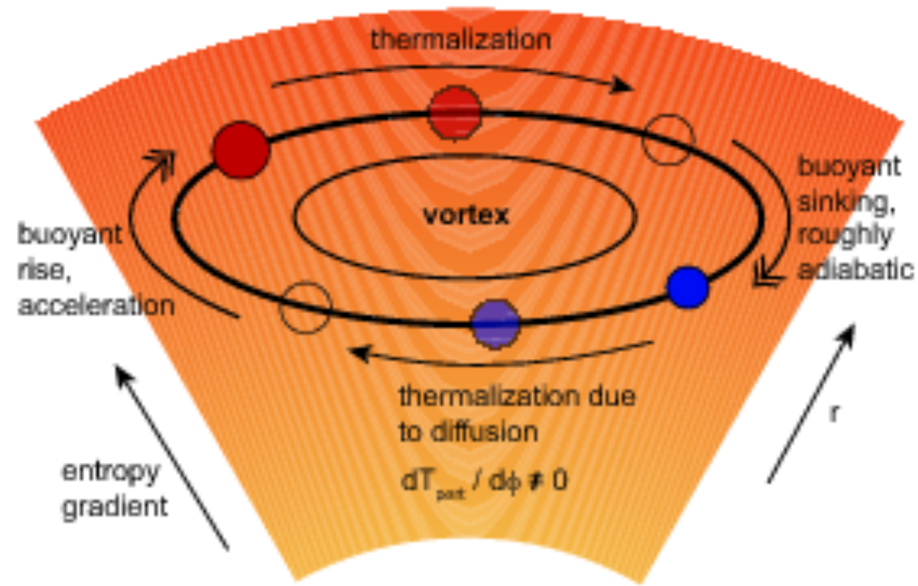

Armitage (2010)

Zombie Vortex Instability

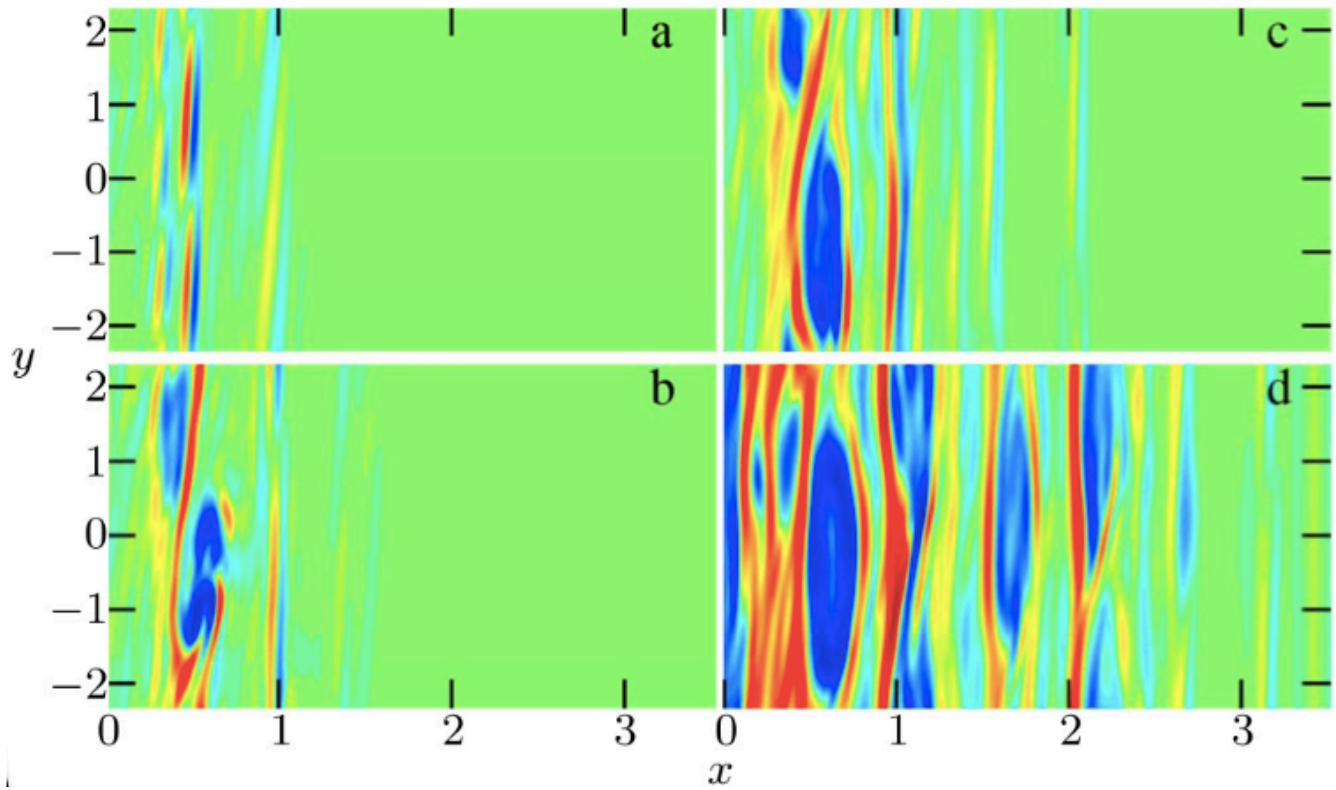

Like playing guitar. If the same note exists in two different strings, if you pluck one of the strings, the other one moves too, in resonance.

The same may happen. In (a), an initial perturbation has an epicyclic frequency associated with it. This frequency will find resonance with the buoyancy frequency elsewhere in the disk (b). The process repeats.

Difficult to maintain the 1st perturbation. The process may not exist in real disks.

Marcus et al. (2015, 2016)

Thermal Instabilities

Buoyancy stabilizes.
Needs to keep disk isothermal.

Moderate heat exchange required.
Needs finite cooling time

Resonance with buoyancy frequency. Needs to keep disk adiabatic.

Vertical Shear Instability

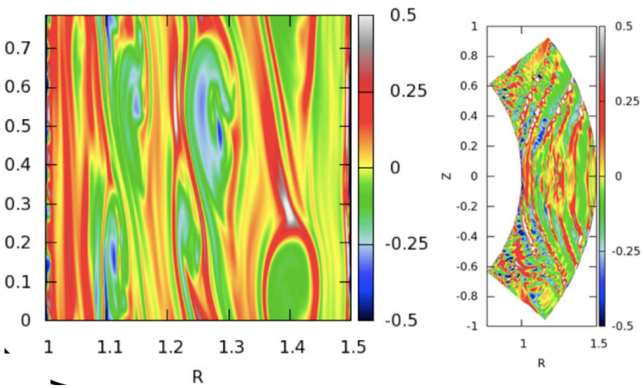

Nelson et al. 2013, Lin & Youdin 2015, Umurhan et al. 2016

Convective Overstability

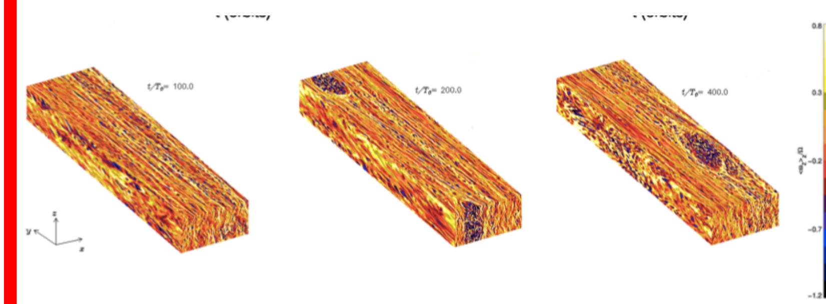

Klahr 2003, Lesur & Papaloizou 2010, Lyra & Klahr 2011, Lyra 2014

Zombie Vortex Instability

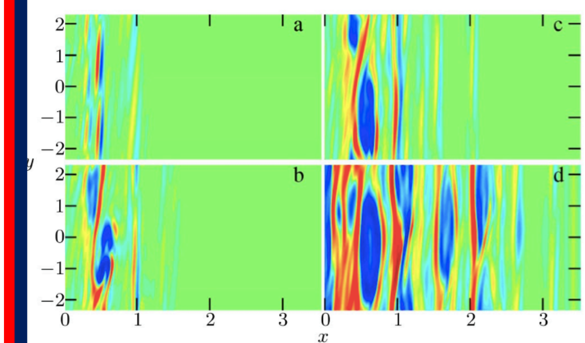

Marcus et al. 2012, 2013, 2015, 2016
Umurhan et al 2016, Lesur & Latter 2016

$\alpha \sim 10^{-4} - 10^{-3}$

$\Omega\tau << 1$
($\kappa < 1$ cm^2/g)

$\alpha \sim 10^{-4} - 10^{-3}$

$\Omega\tau \sim 1$
($\kappa \sim 1$–50 cm^2/g)

$\alpha <\sim 10^{-3}$

$\Omega\tau >> 1$
($\kappa > 50$ cm^2/g)

Opacity

Synthesis

A “butcher diagram” for hydro instabilities.

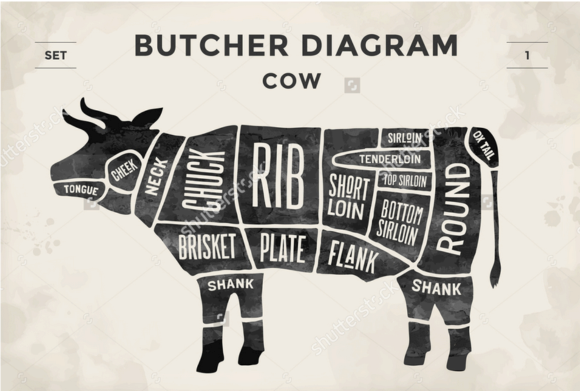

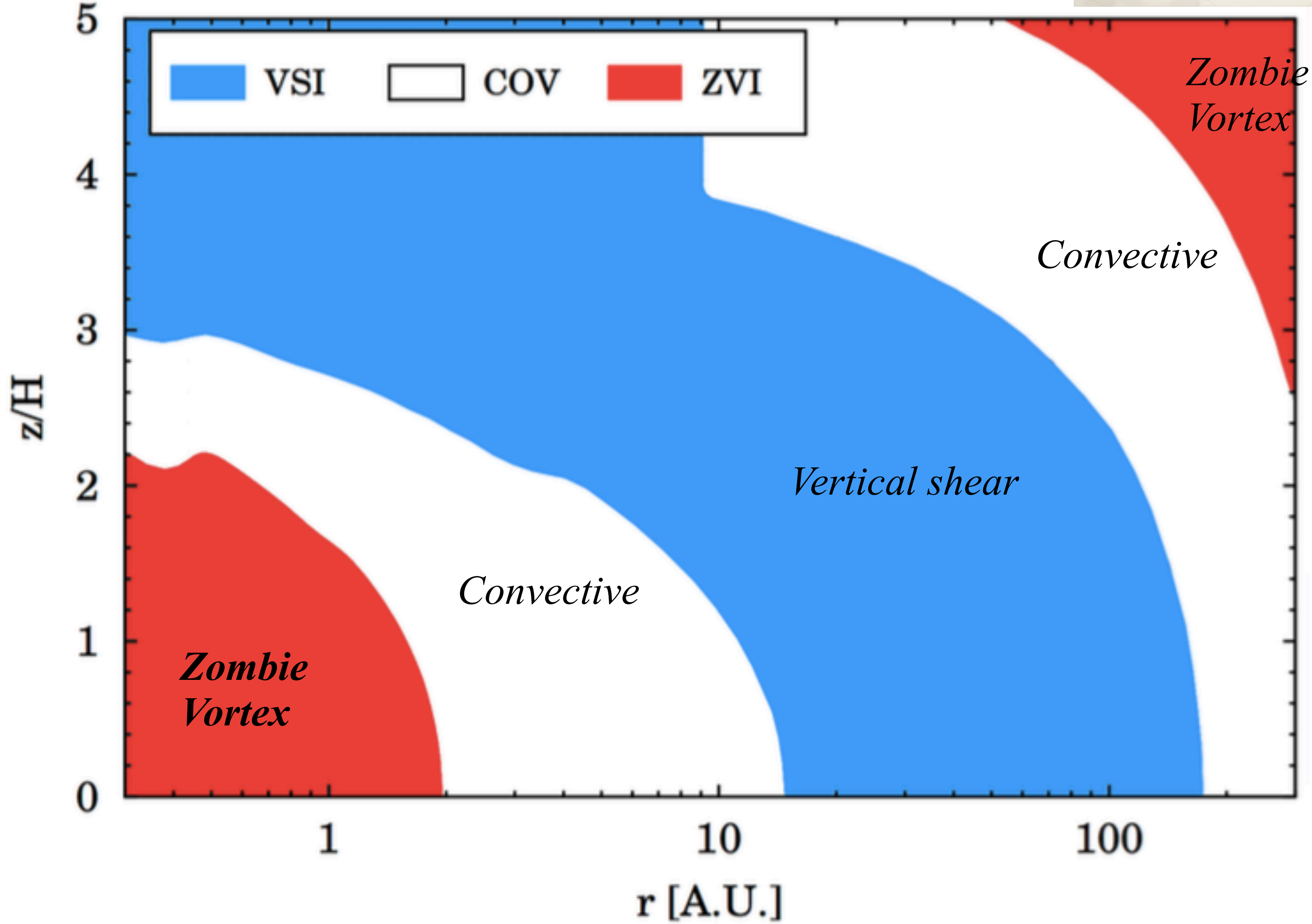

Malygin et al. 2017
Umurhan & Lyra 2017 (review)

Non-ideal MHD: Ohmic, Hall, Ambipolar terms

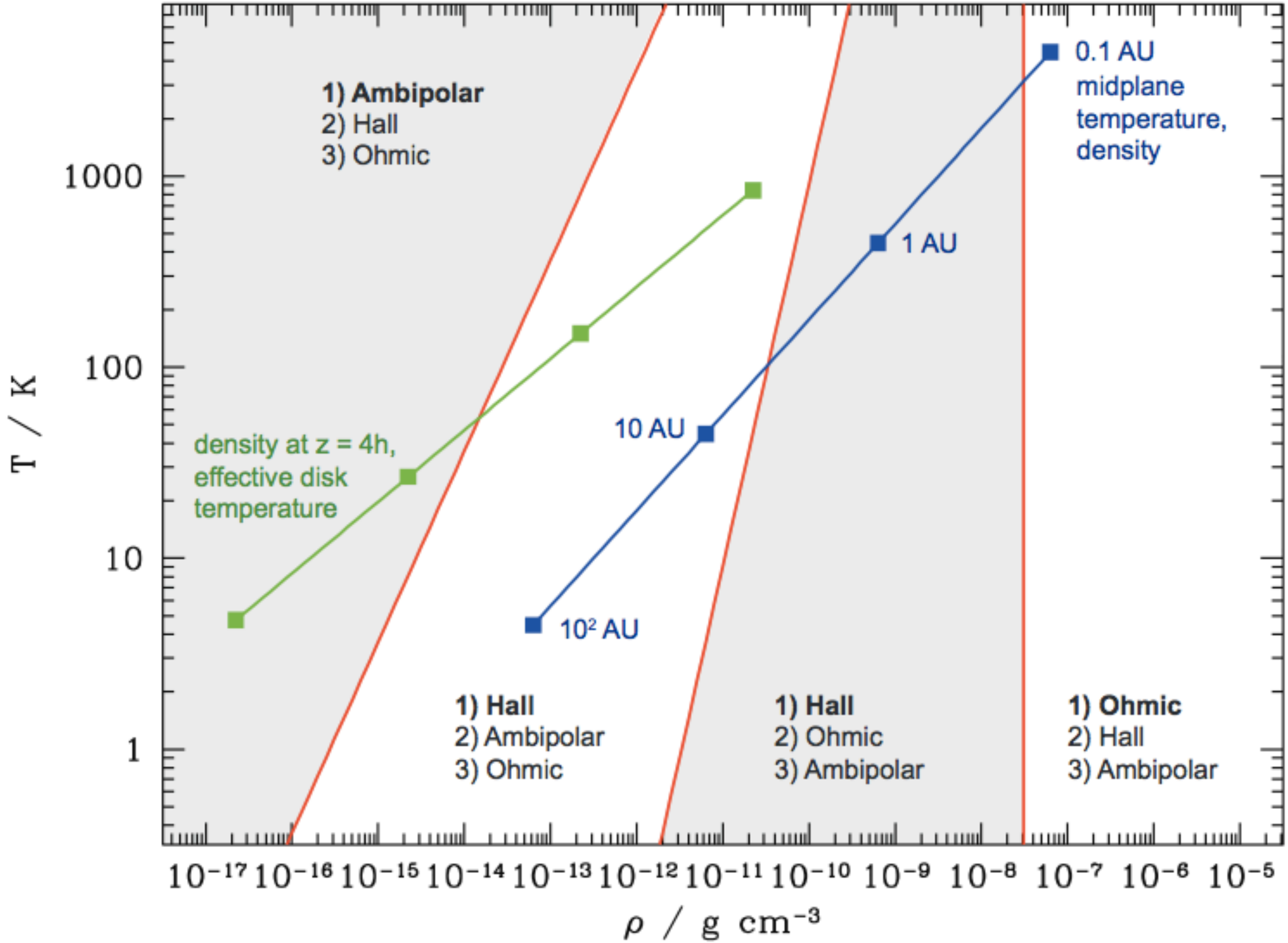

Ambipolar diffusion

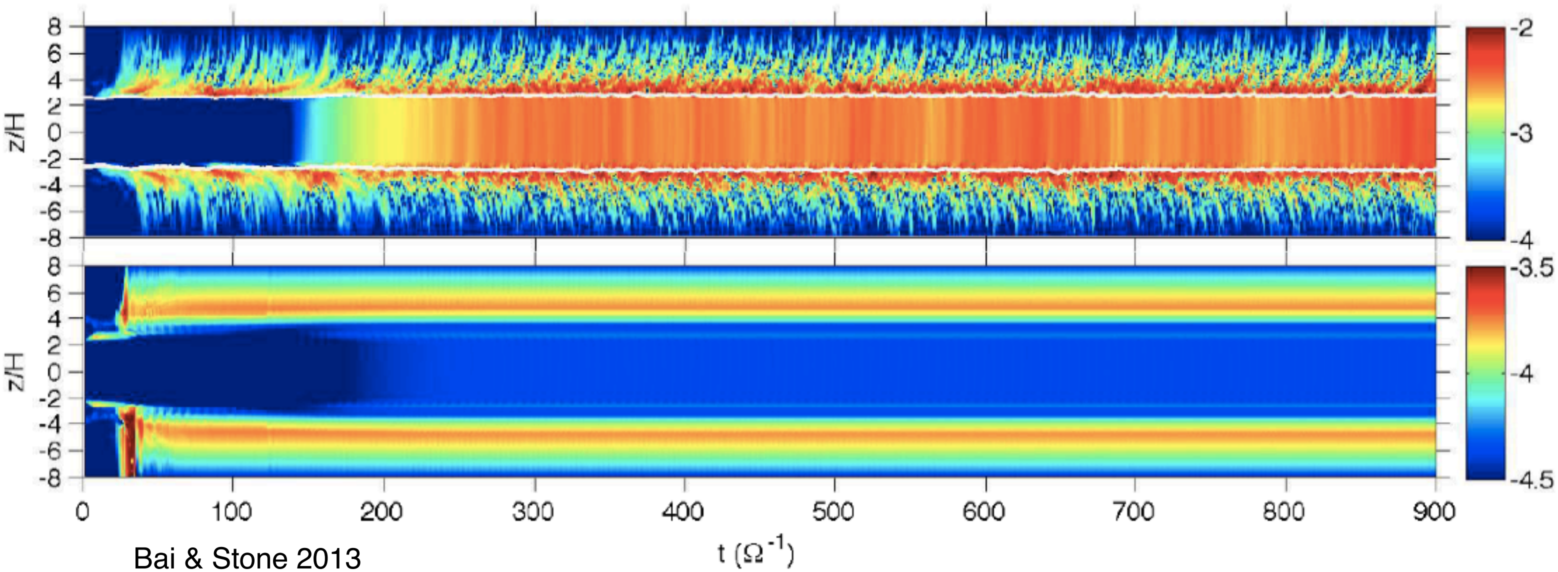

Ohmic

Ohmic + Ambipolar

Bai & Stone 2013

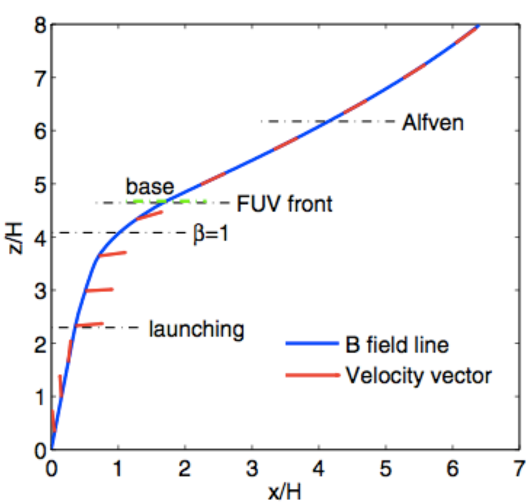

Figure 6. Poloidal field line geometry in our fiducial run OA-b5 (blue solid line). Overplotted are the unit vectors of the poloidal gas velocity (red arrows). The location of the wind launching point, the plasma $\beta = 1$ point, the FUV ionization front, and the Alfvén point are indicated (black dash-dotted). Also marked is the location at the base of the wind (green dashed).

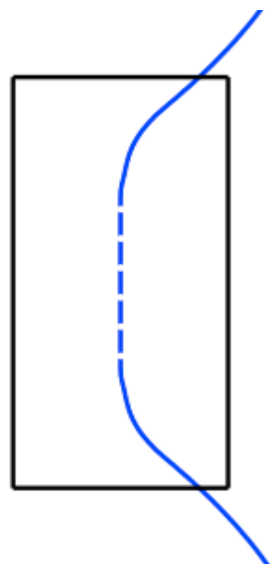

Global Ambipolar + Ohmic

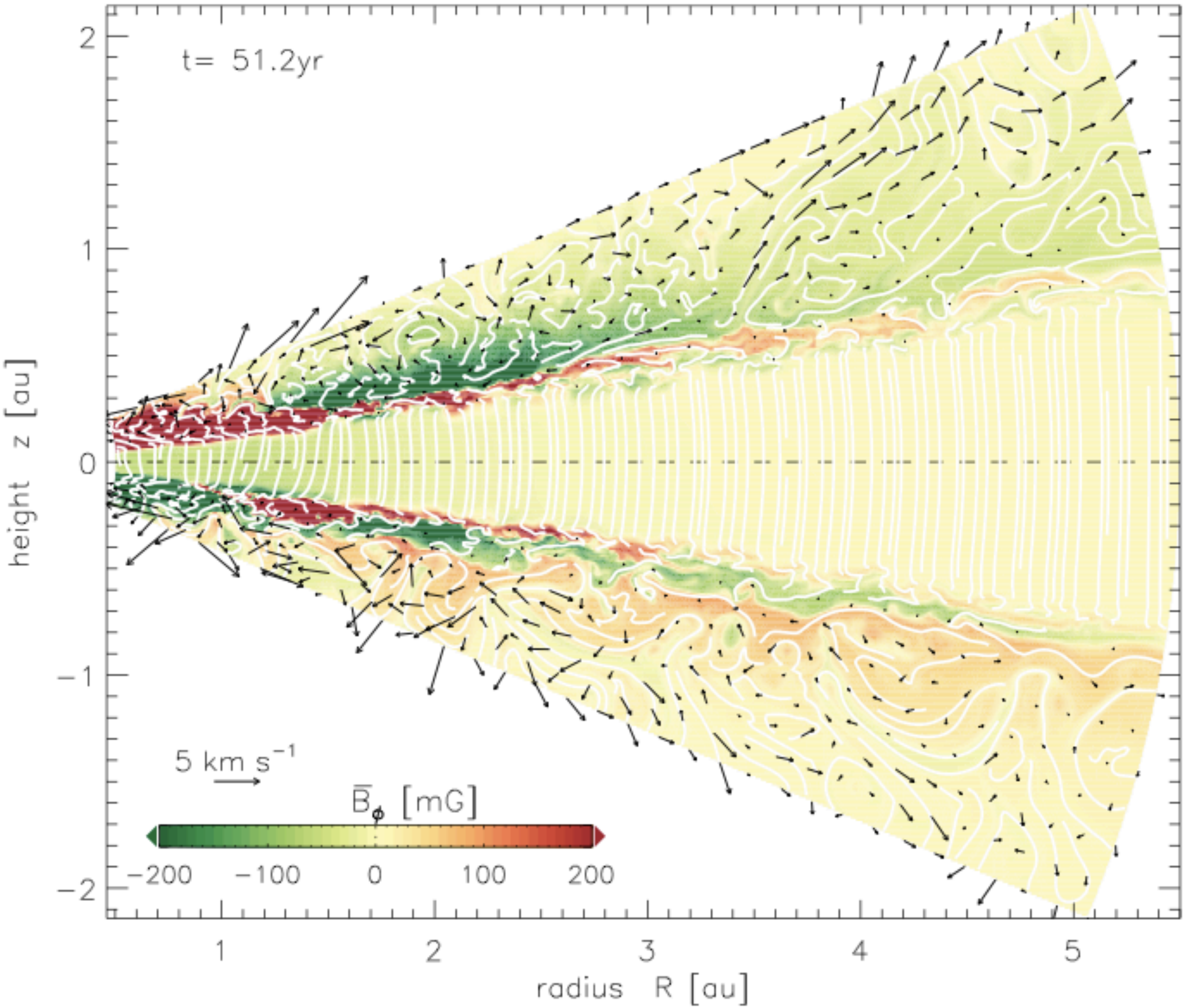

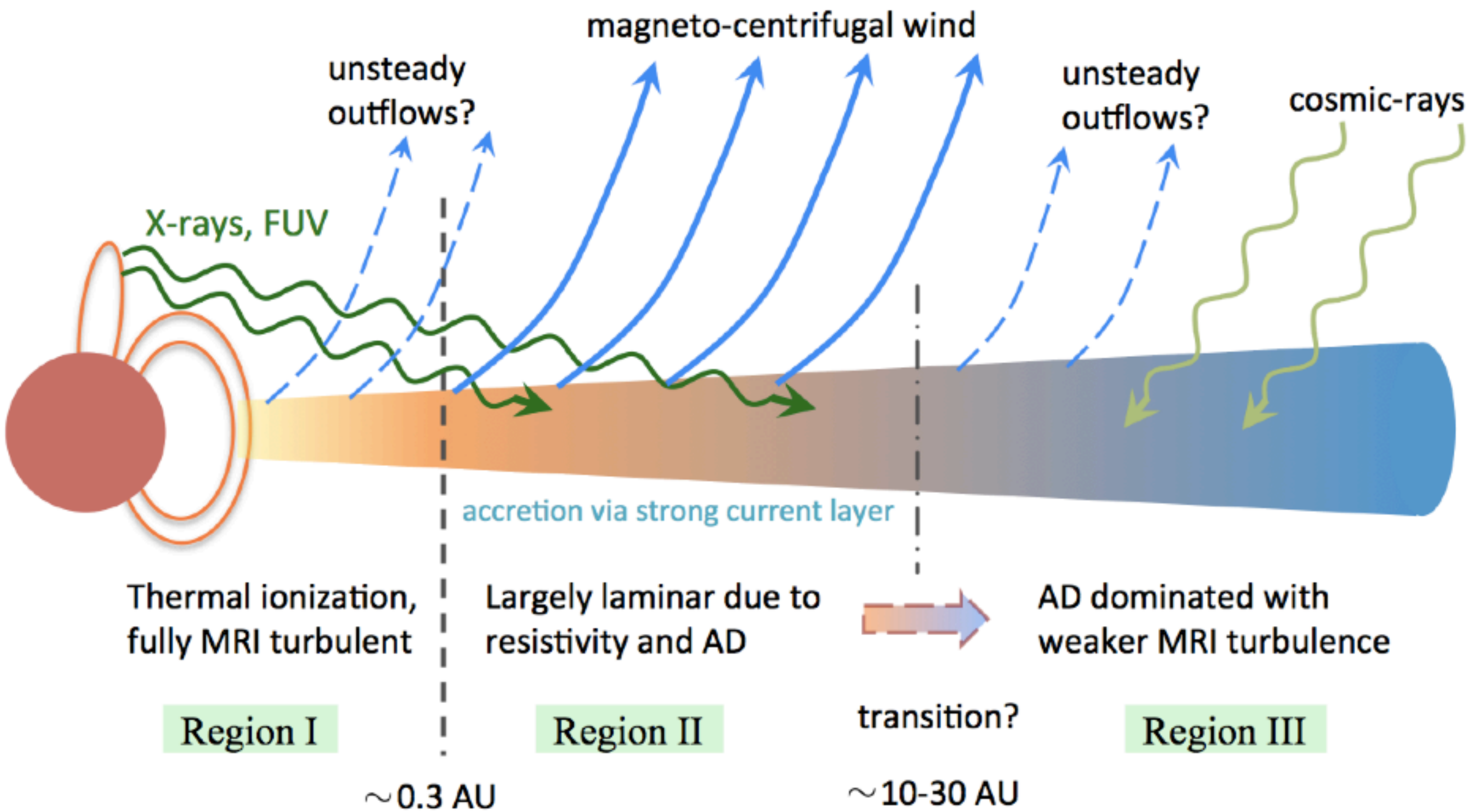
magneto-centrifugal wind
unsteady outflows?
unsteady outflows?
cosmic-rays
X-rays, FUV
accretion via strong current layer
Thermal ionization, fully MRI turbulent
Largely laminar due to resistivity and AD
AD dominated with weaker MRI turbulence
Region I
Region II
transition?
Region III
∼0.3 AU
∼10-30 AU